

# Piezoredox catalysis: a new tool for organic transformations

Hanggara Sudrajat<sup>a,b</sup> and Juan Carlos Colmenares<sup>a</sup>

<sup>a</sup>Institute of Physical Chemistry, Polish Academy of Sciences, Kasprzaka 44/52, 01-224 Warsaw, Poland

<sup>b</sup>National Research and Innovation Agency (BRIN), South Tangerang 15314, Indonesia

Email: [hanggara.sudrajat@brin.go.id](mailto:hanggara.sudrajat@brin.go.id); [jcarloscolmenares@ichf.edu.pl](mailto:jcarloscolmenares@ichf.edu.pl)

Dedicated to Prof. Rajender Varma on the occasion of his remarkable career from the United States  
Environmental Protection Agency

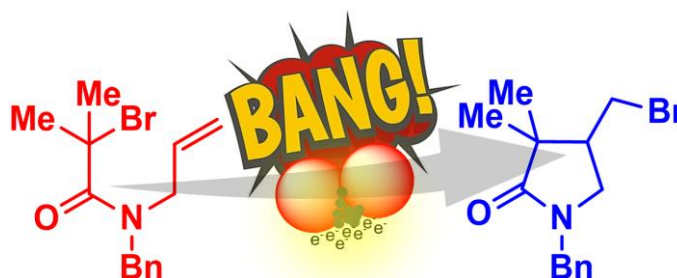
Received 12-15-2024

Accepted 03-27-2025

Published on line 03-30-2025

## Abstract

Piezoredox catalysis exploits the unique properties of piezoelectric materials to drive redox reactions under mechanical stress, combining sonochemistry and mechanochemistry with heterogeneous catalysis as an alternative to traditional methods. By utilizing piezoelectric materials that generate localized electric fields upon mechanical activation, this approach facilitates organic transformations without requiring potential bias, heat, or light. This review discusses the fundamentals of piezocatalysis, the organic transformations it enables, and the strategies for selecting efficient piezocatalysts. It also addresses current challenges and future prospects, emphasizing the potential of piezoredox catalysis to advance synthetic methodologies.



**Keywords:** Mechanical energy, piezoelectricity, charge carriers, catalysis, organic synthesis

## Table of Contents

1. Introduction
  2. Fundamentals of Piezoredox Catalysis
  3. Piezocatalyzed Organic Transformations under Sonication
  4. Piezocatalyzed Organic Transformations under Milling
  5. Piezocatalyzed Organic Transformations under Mixing
  6. SET as a Fundamental Process in Piezocatalyzed Organic Synthesis
  7. Selecting Potentially Efficient Piezocatalysts
  8. Outlook
  9. Conclusions
- References

## 1. Introduction

Piezoelectric materials have recently emerged as important tools in driving redox reactions through an approach termed "piezoredox catalysis," which integrates mechanochemistry with redox chemistry and heterogeneous catalysis to develop alternative pathways for chemical synthesis. This approach utilizes the mechanical activation of piezoelectric materials, such as barium titanate ( $\text{BaTiO}_3$ ), to facilitate redox reactions.<sup>1</sup> The reaction is not driven over the activation barrier by photons (photocatalysis), external potential bias (electrocatalysis), or thermal energy (thermocatalysis) but by mechanical energy from ultrasound or colliding milling items.<sup>2</sup> Unlike mechanochemistry, where activation primarily occurs through shear forces and compression with minor thermal effects, piezoredox catalysis—often called piezocatalysis—relies on mechanical forces to generate localized electric fields, inducing charge transfer. Thus, activation is driven by an internally generated electrical potential rather than direct mechanical effects.<sup>3</sup> Piezoredox catalysis is a subset of mechanoredox catalysis, a broader term for any redox process initiated by mechanical forces. The key distinction is that piezoredox catalysis specifically requires a piezoelectric material. Over the past decade, it has enabled a completely new class of organic transformations.

When subjected to mechanical stress, these piezoelectric materials become polarized and generate localized electric fields, enabling them to participate in redox reactions by donating or accepting electrons. The foundation of piezoredox catalysis is sonochemistry<sup>4</sup> and mechanochemistry,<sup>5</sup> which facilitate chemical reactions through ultrasound irradiation or the grinding of solid reactants. The use of piezoelectric materials, for instance in mechanochemistry, allows redox reactions to occur under ambient conditions with simple equipment, without complex setups or inert atmospheres.<sup>1</sup>

Piezoelectric materials are necessary for mechanically driven reactions due to the inherent inefficiency of energy transfer in mechanical reactors, where a significant portion of energy is lost as heat or through mechanical deformation.<sup>6</sup> While this issue is less pronounced at larger scales, small-scale reactions—ranging from a few milligrams to a kilogram—face unfavorable energy demands. This is especially important in the pharmaceutical industry as fine and specialty chemicals are often synthesized on small scales. To overcome this challenge, recent research has turned to piezoelectric materials to harvest unused energy in these systems.<sup>1</sup> These materials convert the wasted energy into an electron flow, enabling more efficient energy utilization.

In essence, piezoredox catalysis extends sonochemical and mechanochemical principles to redox reactions, utilizing piezoelectric materials that generate a temporary polarized state under mechanical stress. This polarized state allows the piezoelectric material to act as a redox mediator, facilitating redox reactions similar to those in photoredox catalysis. For example,  $\text{BaTiO}_3$  can undergo a redox cycle, reducing a substrate and then returning to its ground state by oxidizing another species.<sup>1</sup> This ability to mimic complex redox mechanisms using force rather than light represents an advancement in synthetic methodology, expanding the range of accessible organic transformations.

Unlike traditional photoredox and thermal redox methods—which often require expensive noble metal catalysts, complex equipment, and substantial energy input—piezoredox reactions can be conducted under ambient conditions using readily available piezoelectric materials, without the need for stringent environmental controls.<sup>1</sup> This simplicity and cost-effectiveness make piezoredox catalysis well-suited for large-scale applications in organic synthesis.

Despite being in its early stages, piezoredox catalysis shows potential for further development and innovation. Future research aims to expand the range of redox transformations adapted to sonochemical and mechanochemical conditions, explore new piezoelectric materials with different surface properties, and integrate piezoredox processes into dual catalytic cycles. These efforts could enhance the versatility of piezoredox catalysis, enabling the handling of more challenging radical precursors. As research in this area evolves, piezoredox catalysis becomes increasingly important in developing new synthetic methodologies, driving innovation and promoting more sustainable practices in the chemical industry.

There are a few review articles on piezoredox catalysis for organic transformations. In 2021, Leitch and Browne briefly discussed piezoredox chemistry, demonstrating how piezoelectric materials like  $\text{BaTiO}_3$  drive radical reactions through mechanical activation, mimicking photoredox catalysis without the need for light or costly noble metal catalysts.<sup>1</sup> This solvent-free, scalable approach enables transformations such as aryl radical formation, ATRC, and trifluoromethylation, offering an air- and moisture-tolerant, industrially viable alternative to traditional redox methods. In 2024, Zeitler and Golder highlighted advancements in piezoredox catalysis for radical polymerization, providing a greener alternative to traditional thermal or photochemical methods.<sup>7</sup> They discuss key contributions, mechanistic insights, and challenges in ultrasound- and ball milling-driven radical polymerization and crosslinking. In the same year, Jiang and Wang summarized piezoredox chemistry as a powerful tool in organic synthesis, resembling photoredox catalysis by employing piezoelectric materials for radical reactions.<sup>8</sup> Despite being the key component of piezocatalyzed organic reactions, existing reviews unfortunately overlook the crucial aspect of designing potentially active piezoelectric materials. It should be noted that all piezoelectric materials used in piezocatalyzed organic synthesis so far have been commercially available samples, rather than lab-made ones. Engineering these piezocatalysts could lead to enhanced reaction efficiency and expanded synthetic possibilities. Thus, this review article offers an updated, state-of-the-art discussion on piezocatalyzed organic synthesis while also covering the materials aspect. Our goal is to bridge the gap between materials scientists developing piezoelectric materials for organic synthesis and organic chemists seeking to understand the material aspect of piezocatalysts. By integrating the design of piezoelectric materials with targeted organic transformations, such as matching the redox potential between the piezocatalyst and the target reaction, we aim to establish a common language that fosters effective collaboration between materials scientists and organic chemists.

In the following section, we discuss the fundamentals of piezoredox catalysis, detailing how piezoelectric materials function as heterogeneous catalysts in mechanically driven redox reactions. We explore the underlying mechanisms that enable these materials to facilitate electron transfer under different mechanical stresses, including sonication, milling, and mixing. The discussion also covers the influence of

factors such as pressure, frequency, and material properties on catalytic efficiency. We then highlight reported works in chronological order, followed by recent advancements in the field, demonstrating the potential of piezocatalysis in various organic transformations.

## 2. Fundamentals of Piezoredox Catalysis

The fundamental principle behind piezoredox catalysis, often referred to as piezocatalysis, is the ability of certain materials to generate electrical charges when subjected to mechanical stress, such as bending, stretching, or compressing.<sup>9, 10</sup> These piezoelectric materials can convert mechanical energy into electrical energy, which can then be harnessed to facilitate chemical transformations. Mechanical energy sources can vary. Traditionally, tools like a mortar and pestle or a hammer were used for generating mechanical force, but modern approaches rely on more reproducible methods, such as sonication horns, ultrasonic baths, ball mills, and bench-top vortexers.<sup>7</sup> Sonication (ultrasonic irradiation) is frequently employed in chemical reactions. It uses ultrasound waves to generate and collapse cavitation bubbles, creating shear forces within the reaction mixture.<sup>11</sup> Ultrasonic horns concentrate energy on a small area with greater intensity compared to ultrasonic baths, which apply force more broadly and are more widely accessible.<sup>12</sup> Ball mills provide another option, utilizing a sealed jar containing ball bearings that is agitated to transfer kinetic energy to the reactants through impacts. Unlike methods that depend on solvents for energy transfer, ball milling can operate efficiently in the solid state or with minimal solvent, a technique referred to as liquid-assisted grinding (LAG),<sup>5</sup> which improves mixing and solubility using only trace amounts of liquid.

A piezoelectric material cannot be classified as a piezocatalyst unless it demonstrates catalytic activity. While such a material may generate electrical energy upon applying external mechanical force, it might not be capable of driving chemical reactions, particularly if the target reaction is kinetically sluggish or thermodynamically unfavorable. To confirm whether a piezoelectric material functions as a piezocatalyst, both its piezoelectric properties and catalytic activity must be assessed under mechanical force. The performance evaluations can then be cross-correlated and cross-referenced. If a material exhibits catalytic activity exclusively under mechanical force and shows piezoelectric behavior, it is considered as a piezocatalyst. Similarly, if a specific reaction occurs only in the presence of a piezoelectric material and mechanical energy input, this reaction can be classified as piezocatalytic. These criteria form the basis for distinguishing piezocatalysts and understanding their role in facilitating unique reaction pathways. This concept is schematically illustrated in Figure 1. Thus far, the examination of piezoelectricity and piezocatalytic activity has been performed independently. This practice can be referred to as indirect cross-correlation between piezoelectricity and catalytic activity, or ex-situ examination. In contrast, in-situ and operando examinations involve measuring piezoelectricity directly within the catalytic system under study as the reaction occurs. However, direct measurement of piezoelectricity during catalytic operation has yet to be realized. Consequently, in many cases, we cannot fully confirm that the observed catalytic behavior is due to the piezoelectric effect.

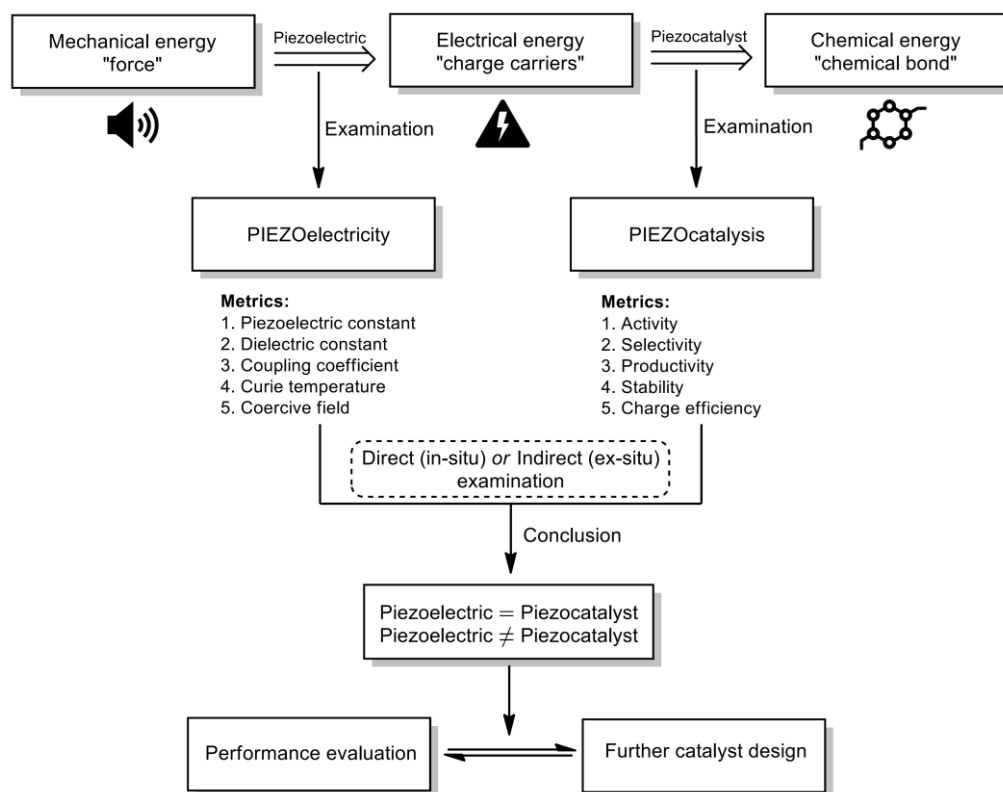


**Figure 1.** Cross-correlation (a quantitative approach for measuring relationships between datasets) and cross-referencing (a qualitative approach for linking and validating information) of the piezoelectricity and catalytic performance.

To understand piezocatalysis, we need to understand the basic concepts of piezoelectricity. Piezoelectricity is a phenomenon observed in certain crystalline materials that lack a center of symmetry.<sup>13</sup> When these materials are mechanically deformed, their internal dipole moments realign, resulting in the generation of an electric field and surface charges. The magnitude of this electric field is directly proportional to the amount of mechanical stress applied to the material.<sup>14</sup> Common piezoelectric materials include lead zirconate titanate (PZT), zinc oxide (ZnO), and BaTiO<sub>3</sub>. In the context of organic synthesis, BaTiO<sub>3</sub> is the most widely used material. It has already been proven effective in facilitating chemical bond formation and in activating small molecules.

The piezocatalytic effect relies on the same principles as piezoelectricity but extends these principles to catalysis. When a piezoelectric material is deformed under mechanical stress, the resulting electric field can induce redox reactions on the surface of the material.<sup>2</sup> This effect is particularly useful for facilitating electron transfer reactions, which are fundamental to many chemical processes. By harnessing mechanical energy, piezocatalysis provides a means to drive reactions without the need for external potential bias, heat or light, making it a potentially more sustainable and energy-efficient alternative to traditional catalytic methods.

The mechanism of piezocatalysis involves several key steps that convert mechanical energy into chemical energy. When a piezoelectric material is subjected to mechanical stress, such as ultrasonic vibration or mechanical grinding, it becomes polarized and generates surface charges.<sup>2</sup> These charges can then participate in redox reactions by either donating or accepting electrons to and from reactant molecules that have been adsorbed on the surface. The two widely accepted mechanisms for elucidating piezocatalytic

phenomena are energy band theory and the screening charge effect.<sup>14</sup> The latter is developed for and typically relevant to piezoelectric materials that are not semiconducting.

The mechanism based on energy band theory describes how piezoelectric materials facilitate catalytic reactions through electronic processes. According to this theory, the electronic properties of materials are defined by their energy band structure, which includes the conduction band (CB) and the valence band (VB). In piezoelectric materials, mechanical stress induces changes in the energy band structure, affecting the charge carriers within the material. When these materials are stressed, an internal electric field is generated, modifying the band structure and shifting the energy levels of the CB and VB. This deformation of the crystal lattice causes a redistribution of electronic states and the creation of localized energy states within the band gap. The induced electric field influences the movement of electrons and holes, exciting electrons in the CB to higher energy states and creating electron-hole pairs. These mechanically excited charge carriers can then migrate to the surface, where they participate in redox reactions. The efficiency of this process depends on the ability of the material to maintain a high density of active charge carriers and facilitate their migration to the reaction sites. Charge migration efficiency can be assessed by the electrical conductivity parameter, which represents charge mobility upon mechanical activation.

The other mechanism, the screening charge effect, emphasizes the roles of piezopotential and external screening charges, which are surface adsorbates from the surrounding environment. Unlike energy band theory, which focuses on internal electronic properties, the screening charge effect highlights the necessity for piezopotential to match or exceed the Gibbs free energy change required for specific chemical reactions. A key distinction of the screening charge effect is that the charges involved in the redox reactions are not the internal charges of the material but rather the surface-adsorbed screening charges from the surrounding environment. This external charge contribution is important for facilitating the catalytic process, as it directly interacts with the piezopotential generated by mechanical stress. Therefore, the electrochemical properties of the reaction medium are crucial, and the redox properties can be tuned by governing the solvent properties. Understanding this mechanism is fundamental for optimizing piezocatalysis, ensuring that the piezopotential effectively drives the desired chemical reactions by utilizing the external screening charges.

The piezocatalytic mechanisms are schematically illustrated in Figure 2A. In energy band theory, charge carriers are generated internally through mechanical activation, which excites electrons from the VB to the CB, similar to photocatalysis. Thus, the bandgap energy and band edge levels determine the catalytic activity. In contrast, the screening charge effect involves charge carriers originating externally from the environment. Therefore, solvent properties play a crucial role. The piezopotential directly contributes to catalytic activity, making this mechanism analogous to electrocatalysis but without the need for an external potential bias. In the context of piezoredox catalysis in organic synthesis, there is still no consensus on whether the chemical transformations follow energy band theory or the screening charge effect. Organic chemists tend to take a practical approach, focusing on improving synthesis efficiency by optimizing reaction conditions—such as the choice of substrate, solvent, additives, and oxidants—rather than engineering piezocatalysts to enhance piezoelectric effects or uncovering the underlying mechanism at play. A simplified representation of piezoredox transformations in organic synthesis is shown in Figure 2B, resembling the well-established mechanisms of photoredox catalysis.<sup>15</sup>

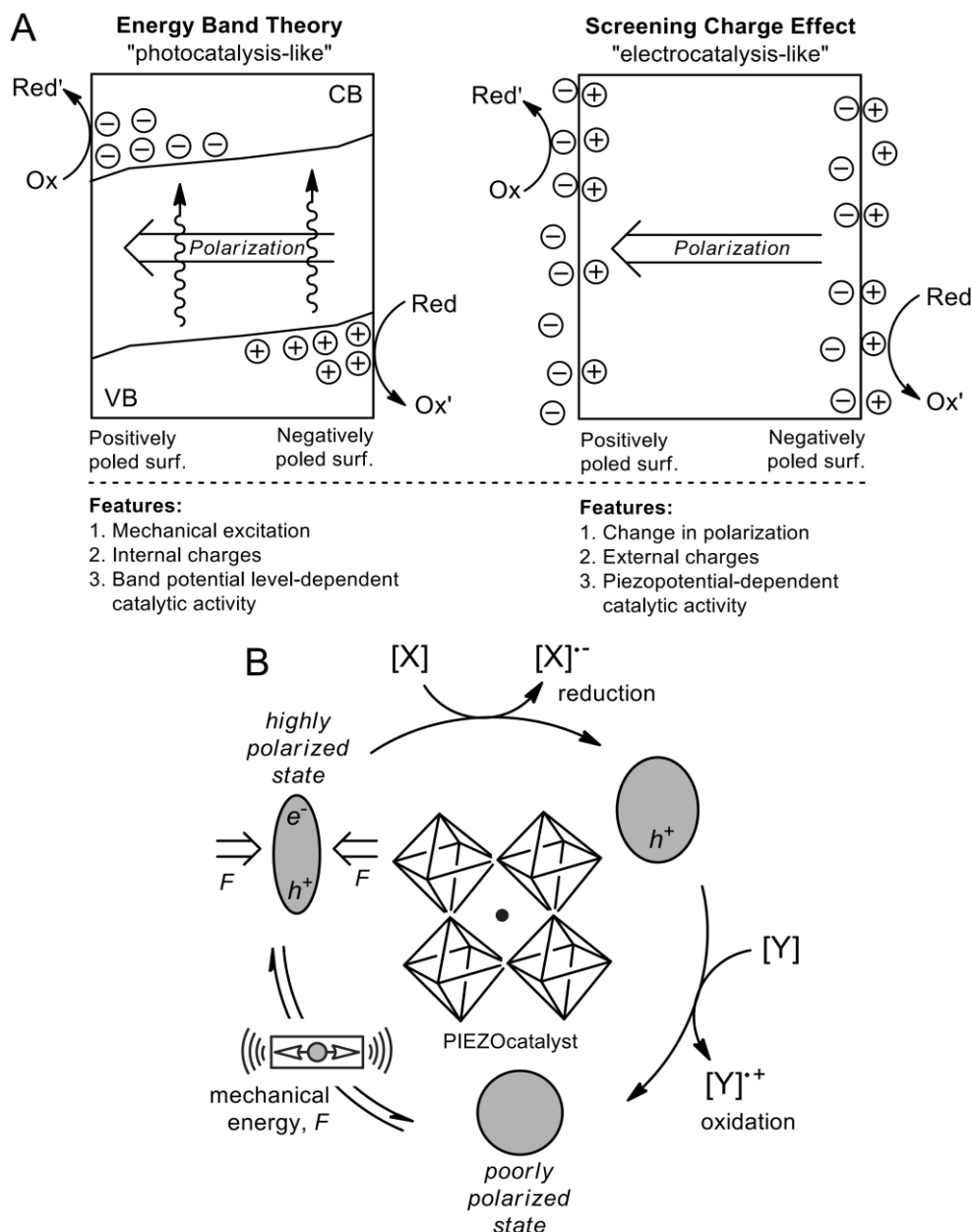


**Figure 2.** (A) The two piezocatalytic mechanisms, with energy band theory being the more widely adopted. Based on the energy band theory, band bending results in contradictory effects. While electrons and holes are spatially separated—accumulating on opposite sides of the poled surface and thereby reducing the probability of recombination—their redox potentials decrease. Electrons become less negative, while holes become less positive. (B) Redox cycles within the mechanoredox framework facilitated by a piezoelectric particle.

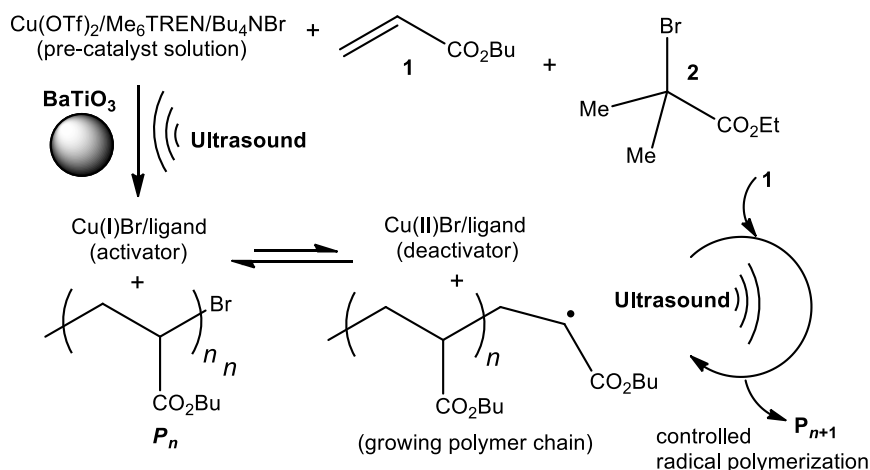
The mechanism underlying piezocatalysis has been a topic of discussion within the catalysis community, particularly in terms of how it compares to photocatalysis and electrocatalysis.<sup>14</sup> Much of the current focus has been on distinguishing or validating these mechanisms, with attention directed toward understanding the pathways of carrier excitation and the influence of piezoelectric potential. Despite these efforts, definitive evidence to thoroughly elucidate the complex processes driving piezocatalysis remains limited, leaving many aspects of its operation unresolved. In the following section, we will discuss reported

studies on the use of piezoelectric materials to drive various organic transformations. This discussion is categorized according to the source of mechanical energy: ultrasound and mechanical vibration (ball milling).

### 3. Piezocatalyzed Organic Transformations under Sonication

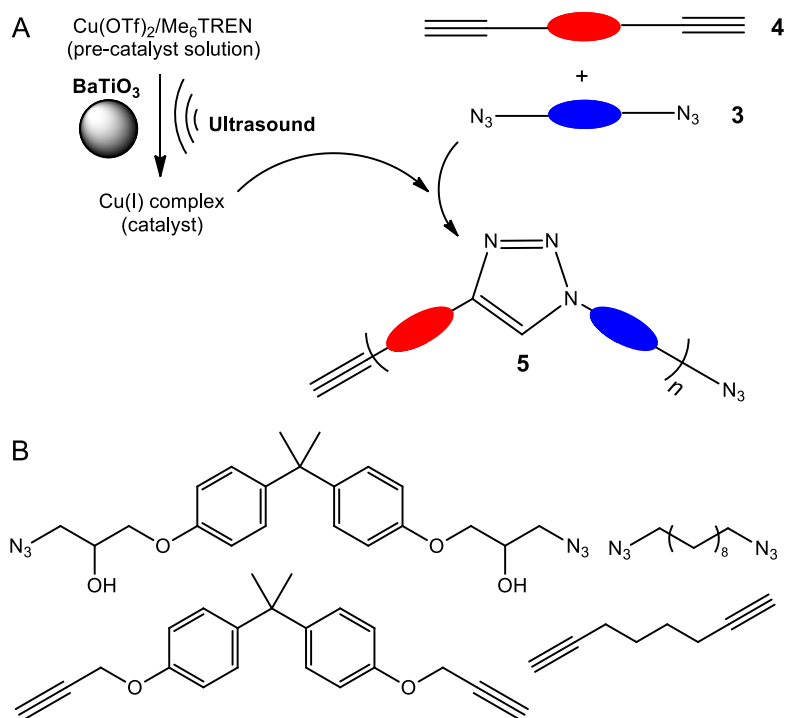
Piezoelectric materials can catalyze redox reactions under mechanical force, such as low-frequency ultrasound or strong mechanical vibration. This force induces charges within the material, generating a strain-induced voltage that facilitates electron transfer with substrates. In piezoelectric materials, aligned dipoles respond to compressive or tensile forces by creating a net charge and a corresponding voltage. When vibrated with ultrasound, piezoelectric materials such as ZnO and BaTiO<sub>3</sub> can generate the electrochemical potential needed for water splitting ( $E^{\text{red}} = -1.23$  V), producing H<sub>2</sub> and O<sub>2</sub> without undergoing decomposition or redox change.<sup>16</sup> This method is distinct from traditional sonochemical processes and may offer a low-cost alternative for water splitting.

For organic transformations, piezoelectric nanoparticles can be used as chemical transducers for the reduction of organic molecules or metal pre-catalysts necessary for coupling reactions or radical polymerizations. In one example, the Esser-Kahn group demonstrated a novel method for controlled radical polymerization (CRP) using ultrasonic agitation to mechanically initiate and control the polymerization process (Scheme 1).<sup>17</sup> BaTiO<sub>3</sub> nanoparticles were used as piezoelectric transducers, which generate an electrochemical potential under ultrasonic agitation sufficient to reduce a Cu(II) precursor to a Cu(I) activator. This process drives an atom-transfer radical polymerization (ATRP) of acrylate monomers, particularly *n*-butyl acrylate **1**, producing well-defined polymers with a narrow molecular weight distribution. The ultrasonic irradiation of BaTiO<sub>3</sub> nanoparticles in the presence of the Cu(II) precursor effectively reduces the metal complex, leading to the initiation of polymerization. The polymerization proceeded with first-order kinetics, and the polymer chain length was observed to grow linearly with time, a hallmark of controlled polymerization. Control experiments showed that the presence of BaTiO<sub>3</sub> nanoparticles and ultrasonic irradiation were both necessary for successful polymerization, as the absence of either led to the formation of only short oligomers or no polymer at all. This result confirmed that the polymerization was not simply due to thermal effects from cavitation but was indeed mediated by the piezoelectric nanoparticles. Further analysis suggested two potential mechanisms: the direct piezocatalytic reduction of the Cu(II) precursor or the generation of radicals through electron transfer from the piezocatalyst nanoparticles. Both mechanisms would lead to the formation of the Cu(I) activator necessary for ATRP. The study also explored the possibility of pre-generating the activator through sonication, but it was found that continuous ultrasonic activation was necessary to sustain the polymerization, indicating that the activator is produced and consumed rapidly in-situ. The polymerization could be paused by stopping the ultrasonic agitation and resumed later without significant loss of control over the molecular weight distribution. This property is similar to other forms of CRP, where the polymerization can be turned on and off by controlling the external stimulus. On the whole, the study introduces a novel, mechanically controlled CRP method using ultrasonic agitation and piezoelectric nanoparticles to initiate and regulate polymerization. The process demonstrates an ATRP-like mechanism, though the exact details of the activation process remain to be fully elucidated. The findings open new possibilities for using environmental vibrations or other mechanical stimuli to create mechanically responsive materials and extend the scope of CRP in polymer chemistry.



**Scheme 1.** Ultrasound-controlled radical polymerization of  $n$ -butyl acrylate **1** occurs through the sonochemical reduction of the  $\text{Cu}(\text{II})/\text{Me}_6\text{TREN}$  complex ( $\text{Me}_6\text{TREN}$ : Tris[2-(dimethylamino)ethyl]amine) at the interface of piezoelectric  $\text{BaTiO}_3$  nanoparticles, which generates the activator for ATRP. The polymerization process begins with the alkyl bromide initiator **2**, and the monomer **1** is added in a controlled manner to the growing polymer chain  $P_n$ . The final polymer  $P_{n+1}$  is obtained following the termination of the chain. Here,  $P_n$  refers to a polymer chain with a polymerization degree of  $n$ .

In another example by the same research group, ultrasound-promoted copper-catalyzed azide **3**-alkyne **4** cycloaddition (CuAAC) reactions were successfully demonstrated to facilitate step-growth polymerization and polymer crosslinking (Scheme 2), processes that are traditionally limited by the need for thermal or chemical activation.<sup>18</sup> They utilized piezoelectric  $\text{BaTiO}_3$  nanoparticles to convert mechanical energy from ultrasound into the electrochemical activity necessary to reduce a  $\text{Cu}(\text{II})$  precursor to an active  $\text{Cu}(\text{I})$  catalyst, thereby driving the CuAAC reaction. The controlled synthesis of linear polytriazoles and crosslinked polymers was realized using mechanical energy instead of heat or light. The ultrasound-promoted CuAAC reaction can effectively induce step-growth polymerization, producing polytriazoles **5** with high molecular weights (up to 18 kDa) and high conversion rates (over 95%) within 24 h. However, challenges related to solubility were identified, as certain polymerization reactions resulted in shorter polymers due to the precipitation of insoluble products. The reaction kinetics followed typical step-growth polymerization patterns, with significant increases in molecular weight occurring only at high monomer conversion levels. The presence of both the  $\text{Cu}(\text{II})$  precursor and  $\text{BaTiO}_3$  was crucial for polymerization, as the absence of either component significantly hindered or entirely prevented polymer formation. A potential background reactivity not mediated by piezocatalysis was also demonstrated, which could be attributed to non-specific homolytic bond cleavage in the solvent or ligand used. In addition to linear polymerization, the crosslinking of polymers through the mechano-click reaction was explored. A polyurethane-based polymer with azide groups was crosslinked with tripropargyl amine, resulting in a solid gel that became a tough, rigid plastic after solvent removal. The crosslinking experiments further confirmed the necessity of the  $\text{Cu}(\text{I})$  catalyst generated via piezochemical reduction for effective crosslinking, as control experiments without the  $\text{Cu}(\text{II})$  precursor failed to produce significant crosslinking. The findings suggest that while the approach is promising, further optimization is needed to address issues like solubility and background reactivity to fully realize the potential of ultrasound-mediated polymer chemistry.



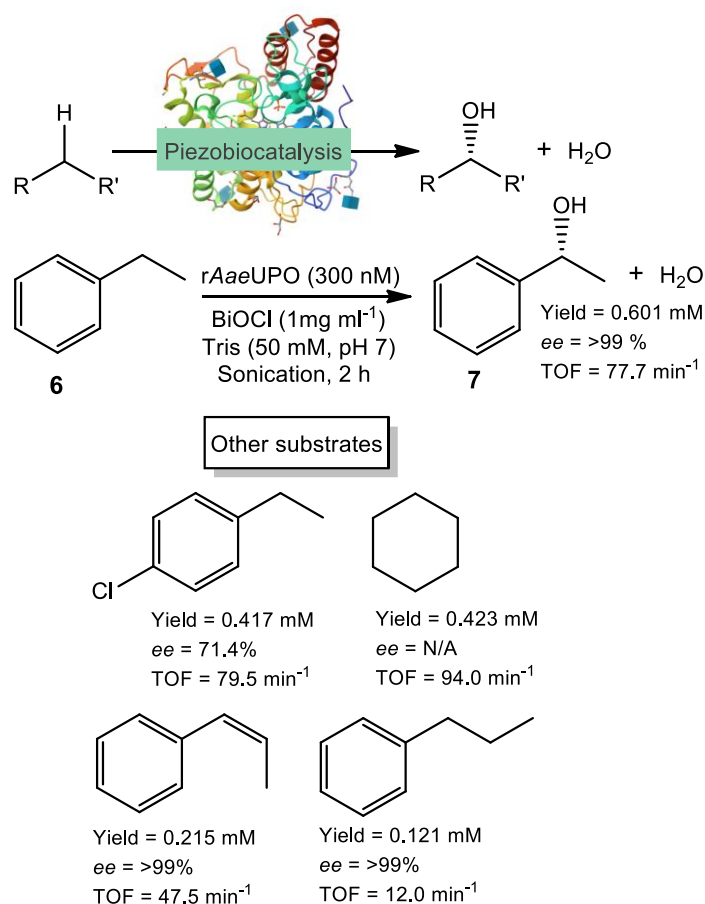
**Scheme 2.** (A) Illustration of the 'Click' polymerization process catalyzed by Cu(I), which is produced via ultrasonic reduction of the Cu(II) precursor ( $\text{Cu}(\text{OTf})_2/\text{Me}_6\text{TREN}$ ). The reaction mixture includes a divalent azide **3**, a divalent alkyne **4**, substoichiometric Cu(II) precursor salt with the ligand  $\text{Me}_6\text{TREN}$ , and piezoelectric  $\text{BaTiO}_3$  nanoparticles. Upon ultrasonic activation, the piezoelectric nanoparticles create an interface where the ligand-stabilized Cu(II) salts are reduced to Cu(I)-based catalysts, facilitating the 'Click' reaction. (B) Structures of the diazides **3** and dialkynes **4** employed in the mechano-click reaction.

In 2019, the Esser-Kahn group further advanced their earlier ATRP research by demonstrating that mechanoredox free radical polymerization (FRP) could be used to produce higher molar mass polymers.<sup>19</sup> By employing a low loading of ZnO, an ultrasound bath, and an Fe catalyst, they achieved polymerization that more closely aligned with the mechanistic characteristics of FRP rather than ATRP. High molar masses ranging from 50 to 340 kDa were obtained with various monomers, although the free-radical process resulted in moderate control over dispersity ( $\mathcal{D} = 1.2\text{--}1.3$ ). Their work also demonstrated the versatility of piezoredox catalysis, including its application in synthesizing block copolymers from macroinitiators.

The Matyjaszewski group then refined the foundational ATRP work conducted by Esser-Kahn and co-workers<sup>17</sup> by adopting more accessible ultrasonic baths in place of sonication horns, enhancing practicality while broadening the range of target molar masses and expanding the monomer scope to include various acrylates.<sup>20, 21</sup> Their innovations extended to piezocatalyst nanoparticles, exploring the effects of size, geometry, and surface ligands, and they introduced ZnO as a lead-free piezoelectric alternative to  $\text{BaTiO}_3$ , further reducing catalyst loading and demonstrating precise temporal control in on-off experiments.

Later, Hollmann and co-workers explored a novel method based on piezoredox to facilitate enzymatic reactions, particularly the oxyfunctionalization of C–H bonds (Scheme 3).<sup>22</sup> Traditionally, such reactions require hydrogen peroxide ( $\text{H}_2\text{O}_2$ ) as a co-substrate. A new method using bismuth oxychloride ( $\text{BiOCl}$ ), which is known to be piezoelectric, was introduced to generate  $\text{H}_2\text{O}_2$  in-situ through ultrasound-driven reactions. This method eliminates the need for external  $\text{H}_2\text{O}_2$  supplies and avoids the use of additional chemical reagents or sacrificial donors, offering an efficient alternative for driving these enzymatic processes. Unspecific

peroxygenases (UPOs) are demonstrated as versatile enzymes capable of catalyzing a wide range of oxidative reactions, such as the hydroxylation of alkanes and the epoxidation of alkenes. These reactions are important for various industrial applications, including organic synthesis and drug development. However, the conventional need for  $\text{H}_2\text{O}_2$  has limited the practical use of UPOs due to difficulties in its controlled production and use. This limitation is addressed by utilizing the piezoelectric properties of BiOCl, which, under ultrasonic stress, can generate reactive oxygen species like  $\text{H}_2\text{O}_2$  directly from oxygen and water.



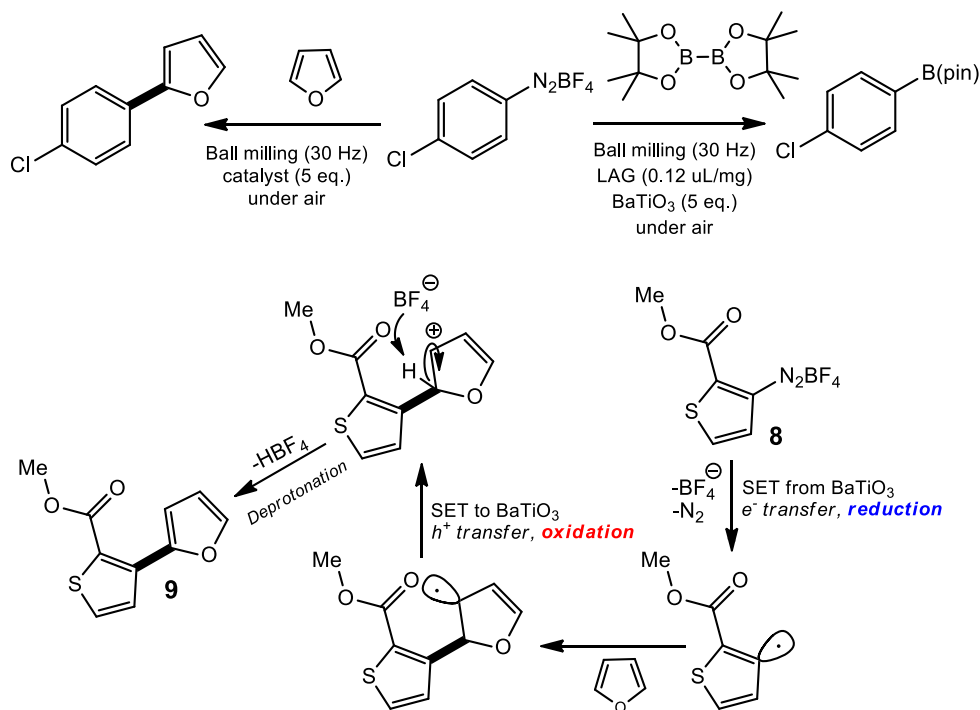
**Scheme 3.** Substrate scope of piezobiocatalytic hydroxylation reactions. The BiOCl-*rAaeUPO* system acts as a platform for converting mechanical energy into chemical energy, enabling peroxygenase-catalyzed transformations under ultrasonic activation. The initial reaction rate and TOF were determined after 15 min of reaction. The reaction conditions included 1 mg mL<sup>-1</sup> BiOCl, 300 nM *rAaeUPO*, and 100 mM substrate ([1-chloro-4-ethylbenzene] = 10 mM) in an oxygen-purged Tris buffer (50 mM, pH 7.0) under ultrasonic irradiation (40 kHz, 70 W, 2 h). N/A = not applicable.

The effectiveness of this piezobiocatalytic approach was evaluated using ethylbenzene and other oxyfunctionalization reactions, including stereoselective benzylic hydroxylation, alkane hydroxylation, and styrene epoxidation. Under ultrasonic conditions, the BiOCl piezocatalyst successfully generates  $\text{H}_2\text{O}_2$  in-situ, enabling the UPO enzyme, *Agrocybe aegerita* (*rAaeUPO*), to catalyze the oxyfunctionalization reactions. The hydroxylation of ethylbenzene **6** to (*R*)-1-phenylethanol **7**, with the enzyme retaining its activity and stability throughout the process. The selective hydroxylation of ethylbenzene to enantiopure (*R*)-1-phenylethanol was accelerated, achieving a yield of 0.601 mM, a turnover frequency (TOF) of 77.7 min<sup>-1</sup>, and an enantiomeric

excess (ee) of >99%. The compatibility and effectiveness of the piezocatalytic system in enzymatic reactions were confirmed. rAaeUPO effectively piezocatalyzed the hydroxylation of propylbenzene (TTN 402, >99% ee), 1-chloro-4-ethylbenzene (TTN 1390, 71% ee), and cyclohexane (TTN 1410), as well as the epoxidation of cis- $\beta$ -methylstyrene (TTN 720, >99% ee) over a 2-h reaction period, producing only trace amounts of overoxidized products. Ethylbenzene exhibited the highest TTN >2000 (>99% ee) and the highest yield (0.601 mM). The findings represent a significant advancement in biocatalysis, providing a greener and more cost-effective alternative for enzymatic oxyfunctionalization. By integrating piezocatalysis with enzyme-driven reactions, the method avoids the drawbacks of traditional H<sub>2</sub>O<sub>2</sub>-based processes, such as the need for external chemical inputs and the associated safety risks. New possibilities are thus opened for expanding the use of piezocatalysis in other types of enzymatic reactions that require reactive oxygen species. This study demonstrates a novel and efficient piezobiocatalytic method that utilizes ultrasound-driven piezocatalysis to generate H<sub>2</sub>O<sub>2</sub> in-situ, facilitating selective enzymatic oxyfunctionalization of C–H bonds. Future research could further optimize piezocatalytic materials, explore their compatibility with a broader range of enzymes and substrates, and integrate this method into scalable continuous flow systems.

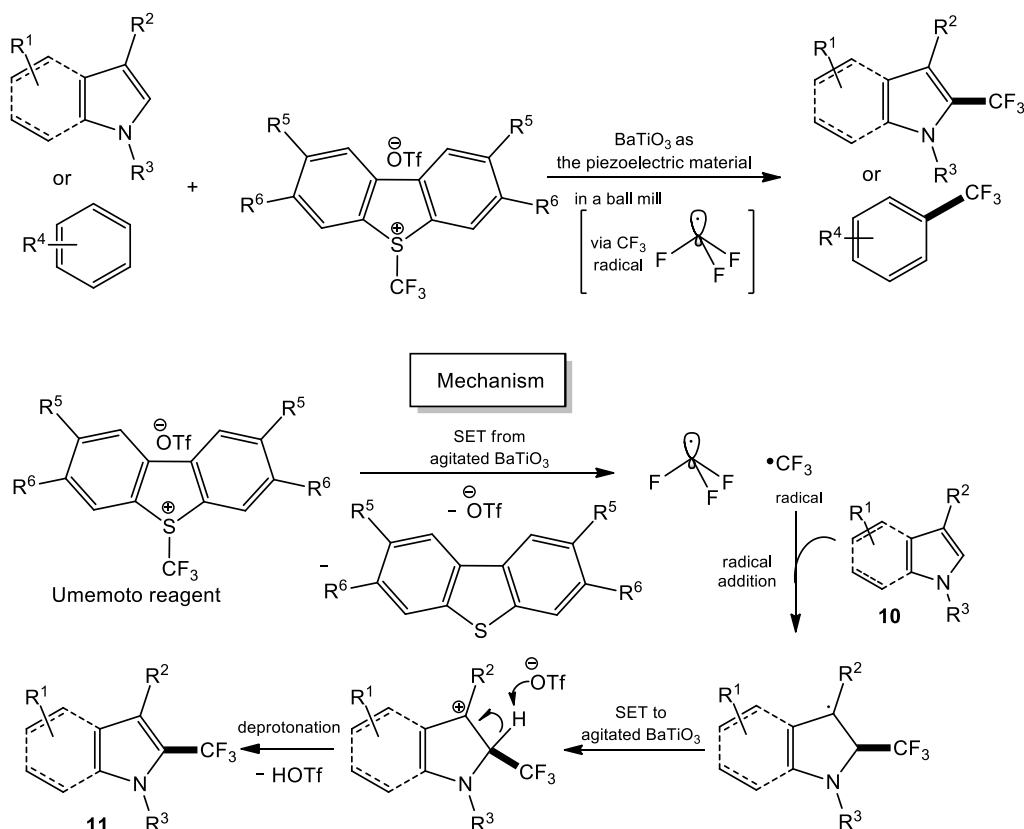
#### 4. Piezocatalyzed Organic Transformations under Milling

In synthetic organic chemistry, mechanical vibration for molecular activation is realized with ball milling. For the first time in 2019, Ito and co-workers demonstrated that ball milling piezoelectric BaTiO<sub>3</sub> could effectively reduce aryl diazonium salts, a common reagent in organic synthesis, through a single-electron transfer (SET) mechanism akin to that in photoredox catalysis.<sup>23</sup> This piezoredox system was successfully applied to perform both arylation and borylation reactions (Scheme 4), such as the C–H arylation of furan, achieving high yields under specific milling conditions. Piezoelectric materials are crucial for these reactions, as the redox processes did not proceed in the absence of these materials or mechanical agitation. The method is also versatile, working effectively with various substrates, including those that are poorly soluble in common solvents. Mechanistic insights suggest that the process involves generating polarized particles through mechanical agitation of the piezoelectric material, which then act as reductants, transferring electrons to the target molecules to facilitate the redox transformation. Reactions do not proceed without the presence of piezoelectric materials and mechanical force. To showcase the practical application of this piezocatalytic method, a gram-scale synthesis of heterobiaryls was explored using the established mechanoredox conditions, along with the recycling of BaTiO<sub>3</sub>. The mechanoredox C–H arylation of furan with **8** was conducted on an 8-mmol scale in a 25-ml stainless steel ball-milling jar containing a single 15-mm diameter stainless steel ball, yielding a heterobiaryl **9** with a 71% yield.



**Scheme 4.** General reaction of the mechanoredox arylation and borylation reactions. Gram-scale mechanoredox arylation of an aryl diazonium salt yielding a heterobiaryl using BaTiO<sub>3</sub> and ball milling.

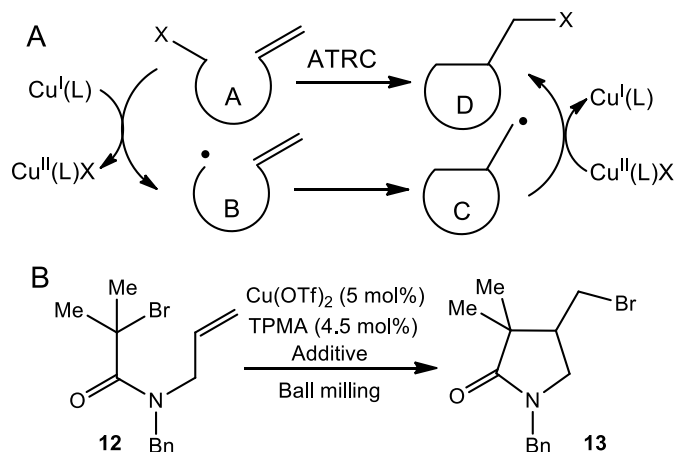
Another elegant work led by Ito and co-workers in 2020 demonstrated the mechanochemical trifluoromethylation of aromatic compounds, which is solvent-free, fast, efficient, insensitive to air, and operationally simple.<sup>24</sup> This method exploits the piezoelectric properties of materials such as BaTiO<sub>3</sub> to generate trifluoromethyl (CF<sub>3</sub>) radicals under solid-state conditions using ball milling. A piezoredox process for C–H trifluoromethylation is introduced, offering an alternative to conventional solution-based methods. This process is particularly important for pharmaceutical chemistry, as the CF<sub>3</sub> group is an important motif that enhances the metabolic stability and pharmacokinetic properties of drugs. When BaTiO<sub>3</sub> is agitated through ball milling, it becomes highly polarized, facilitating charge-transfer reactions that produce CF<sub>3</sub> radicals (Scheme 5). These radicals then participate in radical C–H trifluoromethylation of aromatic compounds **10** yielding trifluoromethylated N-heterocycles **11**. Various conditions and parameters were explored, such as the size of milling balls, milling frequency, and types of piezoelectric materials, to optimize the yield of the desired products. The optimized conditions allowed for the successful trifluoromethylation of a range of indole and pyrrole derivatives, demonstrating the versatility and potential of the proposed method for broad application in organic synthesis.



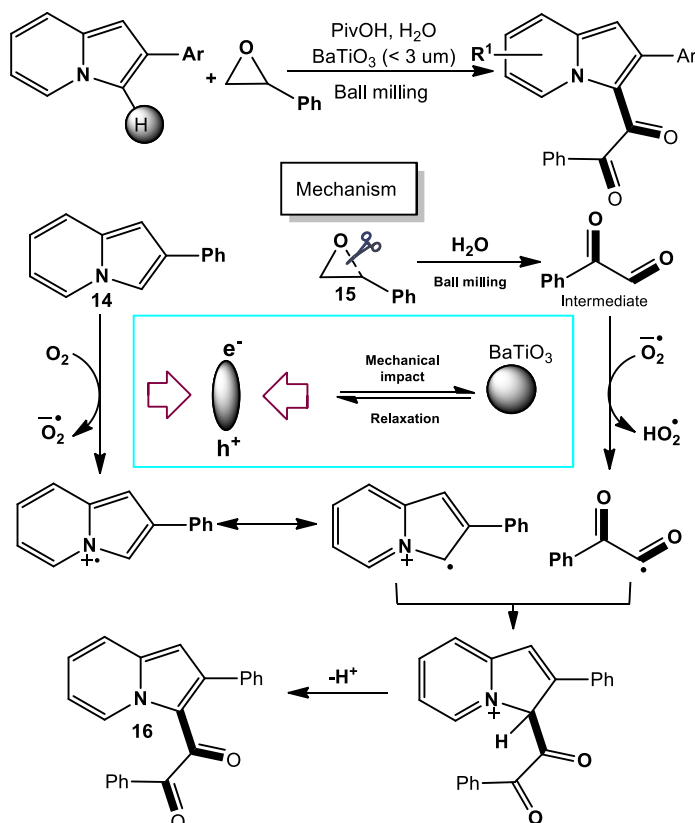
**Scheme 5.** General reaction and mechanism of radical C-H trifluoromethylation of aromatic compounds facilitated by ball milling with piezoelectric materials. Tf represents trifluoromethanesulfonyl.

Meanwhile, the Bolm group investigated a novel approach to copper-catalyzed atom transfer radical cyclization (ATRC) reactions.<sup>25</sup> In ATRCs, copper(I) complexes facilitate the generation of radicals from alkyl halides (A) through reversible redox processes (Scheme 6A). The resulting carbon-centered radicals (B) undergo intramolecular cyclization, forming new C-C bonds to yield products (C). Finally, the in-situ generated Cu(II) complex transfers the halide atom back to (C), producing the corresponding ATRC products (D). This final step ensures the quantitative regeneration of the catalytic Cu(I) species. As shown here, ATRC reactions require high loadings of Cu(I) catalysts or the addition of reducing agents to maintain the presence of the active Cu(I) species. In this study, a new method was explored using the piezoelectric properties of BaTiO<sub>3</sub> to induce redox reactions mechanically, reducing Cu(II) pre-catalysts to active Cu(I) species during ball milling. The ability to control the oxidation state of metal complexes is important in catalysis, particularly for reactions like ATRC. While electrochemistry and light have been employed to achieve redox changes, the study focuses on mechanical energy to induce such transformations. Ball milling is used in conjunction with BaTiO<sub>3</sub>, a piezoelectric material that converts mechanical stress into electrical polarization. This polarization generates an electric field that can reduce Cu(II) to Cu(I) without the need for external electric power. Using BaTiO<sub>3</sub> nanoparticles in a mechanochemical environment can effectively trigger ATRC reactions. Monobromoacetamide was used as the alkyl halide **12**, Cu(OTf)<sub>2</sub> as the copper source, and tris(2-pyridylmethyl)amine (TPMA) as a ligand (Scheme 6B). When these components were milled with BaTiO<sub>3</sub>, complete conversion of the starting material to cyclization product **13** was observed, suggesting successful activation of the Cu(II) catalyst to Cu(I). Both the number and intensity of collisions in the ball mill influenced the effectiveness of BaTiO<sub>3</sub> in catalysis, with higher milling frequencies and larger numbers of balls enhancing

the reaction yield. Non-piezoelectric materials like  $\text{TiO}_2$  and  $\text{Al}_2\text{O}_3$  were ineffective in promoting ATRC under the same conditions. The mechanochemical approach proved advantageous over traditional electrochemical methods, as it does not require an external power supply, simplifying the setup and reducing costs.

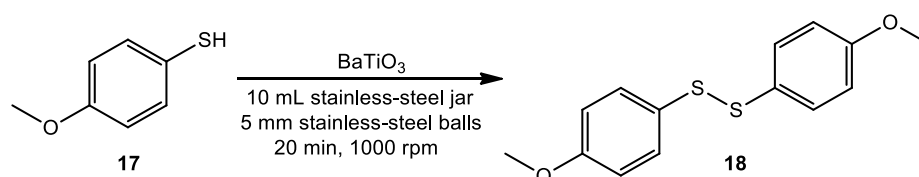


**Scheme 6.** (A) Mechanism of copper-catalyzed ATRC reactions. (B) General reaction of the copper-catalyzed mechanochemical ATRC reaction of **12** carried out with the inclusion of piezoelectric particles.



**Scheme 7.** General reaction and mechanism for the formation of a 1,2-diketoinolizine derivative from an indolizine and an epoxide. Here, styrene oxide **15** undergoes transformation under mechanochemical conditions into a diketo intermediate, which further reacts with 2-phenylindolizine **14** to yield the final product **16**.

In 2021, a scalable, solvent-free method was developed for synthesizing 1,2-diketoindolizine derivatives through mechanochemical processes involving piezoelectric materials (Scheme 7).<sup>26</sup> The study begins by optimizing reaction conditions using 2-phenylindolizine **14** and styrene oxide **15** as model substrates to yield 1,2-diketoindolizine product **16**. The addition of PivOH (pivalic acid) as an additive and BaTiO<sub>3</sub> significantly increased the yield of the product, achieving up to 87% under optimal conditions. Cubic BaTiO<sub>3</sub> was the most effective in facilitating the reaction. Other materials such as ZnO, TiO<sub>2</sub>, and BaCO<sub>3</sub> demonstrated much lower reactivity. The scope of the reaction was tested with various indolizines and styrene oxides. A range of indolizine derivatives, including those with electron-donating and electron-withdrawing groups, successfully underwent the transformation, yielding the desired 1,2-diketoindolizine derivatives in moderate to good yields.

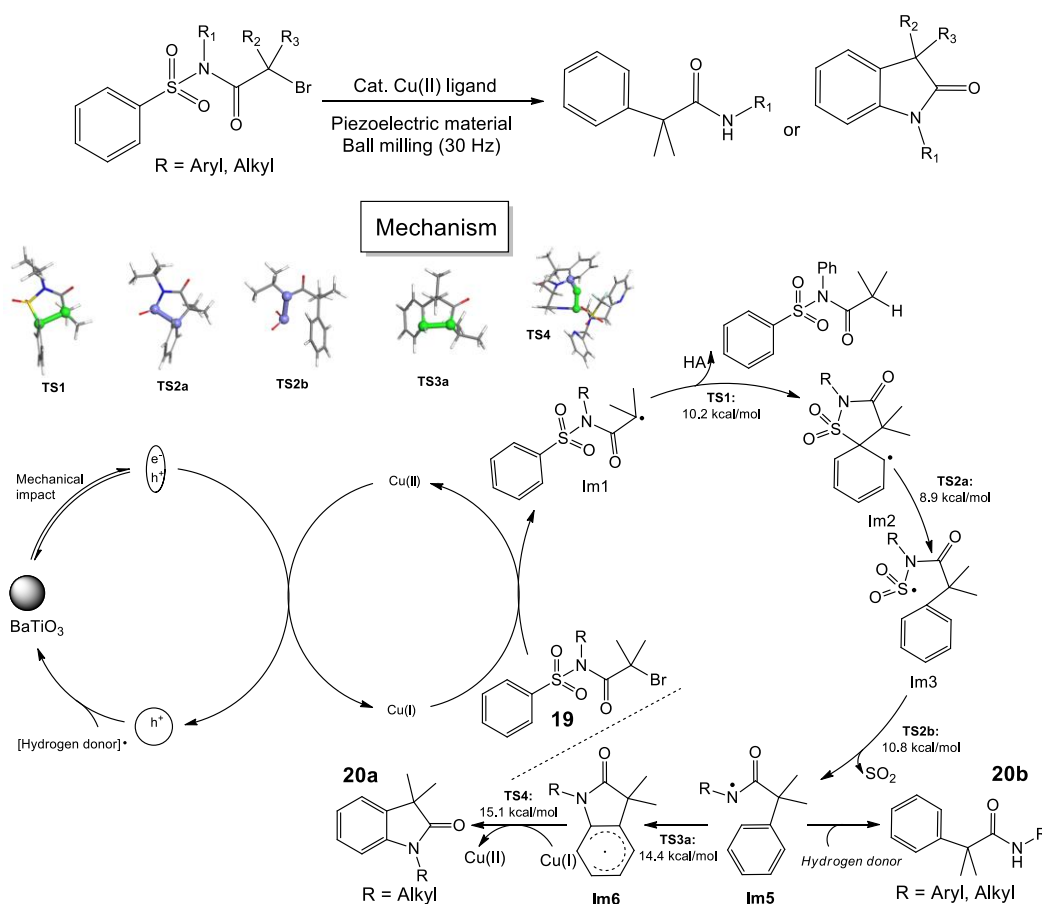


**Scheme 8.** Synthesis of a disulfide product through aerobic oxidation of a thiol.

In 2022, BaTiO<sub>3</sub> was utilized to reduce molecular oxygen through a SET mechanism, facilitating greener oxidative coupling of thiols.<sup>27</sup> Piezocatalysis was exploited for the aerobic homocoupling of thiols. Using 4-methoxybenzenethiol **17** in a mixer mill with BaTiO<sub>3</sub>, switching from zirconia to stainless-steel balls increased the yield of disulfide **18** to 100% in 6 min. PZT also achieved a 95% yield. Without BaTiO<sub>3</sub>, yields dropped significantly. Under nitrogen or with sonication, yields were much lower, emphasizing the need for ball milling and molecular oxygen. A gram-scale aerobic oxidative coupling of **17** using a mixer mill (10 mL stainless-steel jar with five 5 mm stainless-steel balls) was also achieved (Scheme 8). To maintain sufficient oxygen, the jar was opened every five minutes. The desired product **18** was obtained in quantitative yield within 20 min.

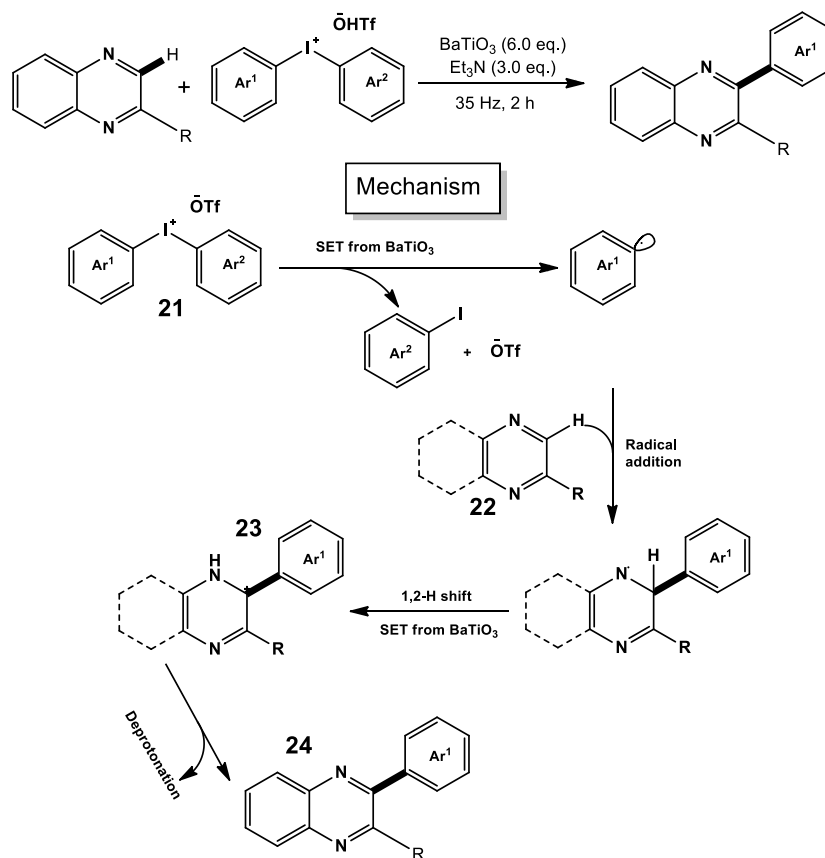
In the same year, Zheng and co-workers investigated the mechanochemical synthesis of oxindoles and  $\alpha$ -arylacylamides using  $\alpha$ -bromo N-sulfonyl amides as starting materials.<sup>28</sup> The reactions are facilitated by a copper(II) pre-catalyst and piezoelectric materials such as BaTiO<sub>3</sub> and PbTiO<sub>3</sub>. The yield of the products ( $\alpha$ -arylacylamides and oxindoles) is significantly influenced by factors such as the amount and type of piezoelectric material, ligand choice, and reaction time. Using BaTiO<sub>3</sub>, the yield of  $\alpha$ -arylacylamides improved substantially, while PbTiO<sub>3</sub> favored the formation of oxindoles with high regioselectivity. The successful synthesis of a variety of  $\alpha$ -arylacylamides and oxindoles was demonstrated with good to excellent yields under optimized conditions. Furthermore, the substrate scope explored demonstrated broad applicability, including substrates with different aryl and alkyl groups as well as those with various electron-withdrawing and electron-donating substituents. BaTiO<sub>3</sub> and PbTiO<sub>3</sub> can be used to selectively synthesize  $\alpha$ -arylacylamides or oxindoles, respectively. The ability to control product formation through the choice of piezoelectric material offers a versatile tool for synthetic organic chemists. Unfortunately, the reason for the change in product selectivity from BaTiO<sub>3</sub> to PbTiO<sub>3</sub> is unknown. If the underlying reasons and the factors related to the inherent properties of the piezocatalyst can be identified, it would enhance the current understanding of catalyst design. Proposed mechanisms for the cascade piezoredox reactions producing oxindoles **20a** or  $\alpha$ -arylacylamides **20b** from  $\alpha$ -bromo N-sulfonyl amides **19** are shown in Scheme 9. The amidyl radical (Im5) can be quenched by hydrogen abstraction to yield the target amides. It is protonated by the LAG additive, such as

acetonitrile, or traces of water in the reaction system, which act as hydrogen donors. In the absence of a LAG additive, Im5 directly forms the radical intermediate Im6 via transition state TS3a.



**Scheme 9.** General reaction of the divergent syntheses of oxindoles and  $\alpha$ -arylacylamides. Mechanism of the piezoredox synthesis of oxindoles and  $\alpha$ -bromo-N-sulfonyl amides **19** facilitated by copper and piezoelectric materials involves a catalytic cycle with free energies relative to Im1, calculated via density functional theory; DFT (kcal/mol). Key transition states (TS1, TS2a, TS2b, TS3a, TS4) are also been proposed to elucidate the mechanism. Im represents a radical species.

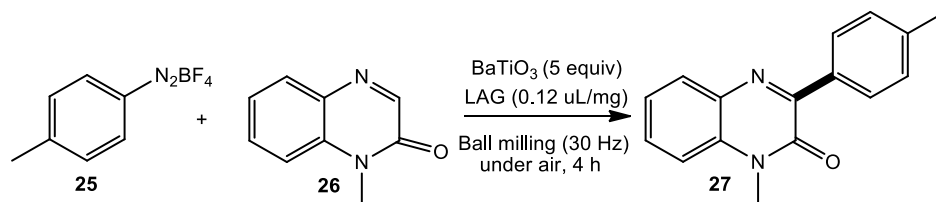
A transition metal-free method for C(sp<sup>2</sup>)-H arylation of quinoxalines was also demonstrated using diaryliodonium salts under mechanically induced conditions, facilitated by piezoelectric BaTiO<sub>3</sub>.<sup>29</sup> Diaryliodonium salt **21** was activated mechanically to generate aryl radical that subsequently reacts with quinoxaline **22** to form the final arylated product **24** via the intermediate **23** after SET reaction driven by BaTiO<sub>3</sub> (Scheme 10). Piezoelectric materials like BaTiO<sub>3</sub> are prerequisite for the reaction, as other non-piezoelectric materials failed to facilitate the target reactions. Optimization of reaction conditions revealed that the use of 6.0 equivalents of BaTiO<sub>3</sub> (<4  $\mu$ m) and 3.0 equivalents of Et<sub>3</sub>N in a ball mill at 35 Hz for 2 h provided the best yields. Different diaryliodonium salts and substituted quinoxalines could be effectively arylated, although some limitations were observed with electron-deficient aryl groups. The piezoelectric effect of BaTiO<sub>3</sub> under mechanical stress plays a key role in generating highly charge-polarized particles capable of reducing diaryliodonium salts via a SET mechanism. Control experiments confirmed the radical nature of the reaction, as the addition of radical scavengers inhibited the product formation.



**Scheme 10.** General reaction and mechanism of the arylation of quinoxalines with diaryliodonium salts.

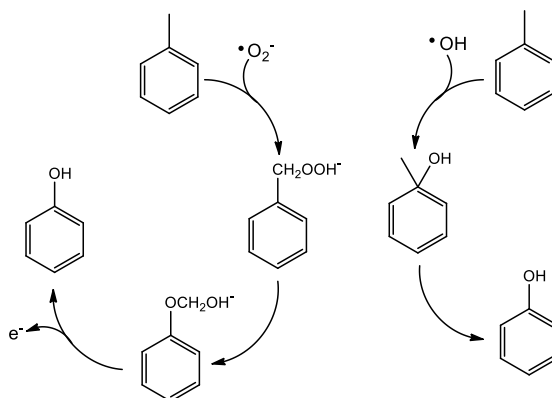
A green synthesis strategy was also demonstrated for producing 2-arylquinoxalines and 3-arylquinoxalin-2(1*H*)-ones via a mechanochemical approach using aryldiazonium salts.<sup>30</sup> This method utilizes ball milling to generate aryl radicals through a SET mechanism induced by mechanical force. The synthesized compounds achieved yields ranging from 28% to 85%, depending on the conditions and substrates used. Initial experiments focused on optimizing the reaction conditions using phenyldiazonium salt **25** and 1-methylquinoxalin-2(1*H*)-one **26** in the presence of BaTiO<sub>3</sub> under ball milling at 30 Hz, yielding the corresponding arylation product **27** (Scheme 11). The initial yield was 22%, which improved to 52% with the addition of acetonitrile as a LAG additive. Other solvents, including DMF and acetone, also contributed to a small improvement in reaction efficiency. Further optimization, including increasing reaction time to 6 h and adjusting the milling frequency, resulted in yields up to 78%. Substituting BaTiO<sub>3</sub> with LiNbO<sub>3</sub> significantly reduced the yield to 34%, demonstrating the critical role of the piezoelectric material in enhancing the reaction efficiency. The substrate scope was expanded to include various aryldiazonium salts and quinoxalin-2(1*H*)-ones with different substituents such as methyl, methoxy, fluoro, chloro, trifluoromethyl, cyano, and nitro groups. The reactions produced moderate to good yields (54%–85%) of the desired 3-arylquinoxalin-2(1*H*)-ones. Similarly, the synthesis of 2-arylquinoxalines was achieved using different aryldiazonium salts and quinoxalines, yielding products in the range of 58%–81%. The reaction also worked with different aromatic compounds like pyrazine and 2,3-dimethylpyrazine, albeit with lower yields (28%–58%). The mechanistic insights gained from control experiments suggest that the reaction mechanism involves a SET process facilitated by piezoelectric materials like BaTiO<sub>3</sub>. This process generates aryl radicals from aryldiazonium salts, which then undergo radical addition and subsequent transformations to produce the final products. The absence of significant product formation without BaTiO<sub>3</sub> or under thermal conditions demonstrates the

importance of mechanical forces and piezoelectric materials. Moreover, the results demonstrate that the reaction conditions, including milling frequency, duration, and the choice of piezoelectric material, significantly impact the yields. Different aryldiazonium salts and quinoxalin-2(1*H*)-ones exhibit varying reactivities, influencing the overall efficiency and yield of the process.



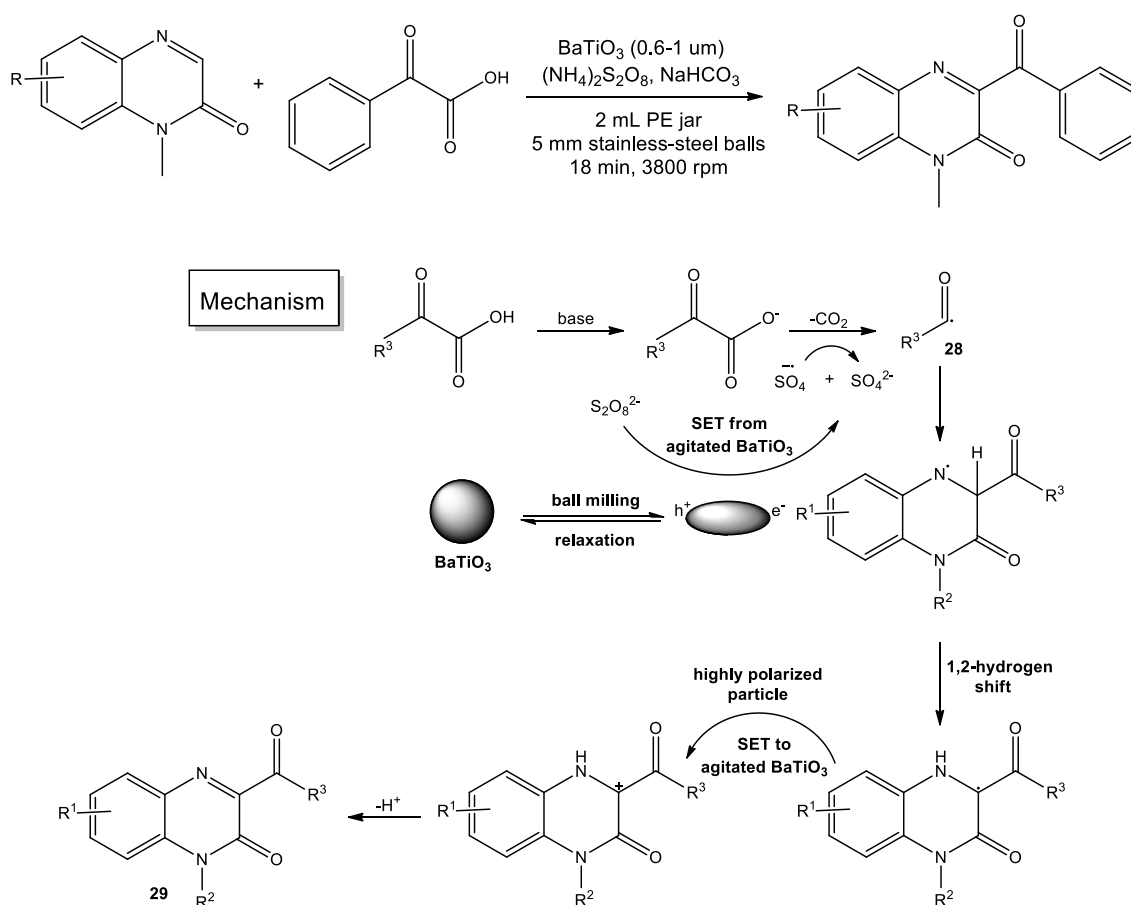
**Scheme 11.** General reaction of the synthesis of 2-arylquinoxalines via aryldiazonium salts.

Later in 2022, the performance of a new piezoelectric material,  $\text{Ba}_{0.75}\text{Sr}_{0.25}\text{SO}_4$  (BSS), in catalyzing the oxidation of toluene to phenol using a ball-milling process was reported.<sup>31</sup> The presence of surface defects and vacancies in BSS was confirmed, and they are believed to increase the catalytic activity of BSS during the ball-milling process. BSS exhibited superior catalytic performance compared to other piezoelectric materials such as  $\text{BaTiO}_3$  and  $\text{SrTiO}_3$ , achieving a phenol yield of 55.6% under optimal conditions. The optimum conditions were determined to be a catalyst dosage of 50 mg, pH of 5, ball-milling speed of 600 rpm, reaction time of 3 h, and a toluene concentration of 0.1 mol/mL. Under these conditions, the oxidation of toluene to phenol was most efficient, with no byproduct formation of benzoic acid, unlike traditional methods. It was proposed that the generation of free electrons and holes on the surface of BSS under external mechanical force leads to the formation of superoxide radicals ( $\bullet\text{O}_2^-$ ) and hydroxyl radicals ( $\bullet\text{OH}$ ), which are primarily responsible for the oxidation process. The superoxide radicals, generated from the interaction of free electrons with oxygen in the air, play a crucial role in attacking the methyl group of toluene, forming toluene hydrogen peroxide, which subsequently rearranges to form phenol under acidic conditions (Scheme 12). Hydroxyl radicals, although secondary in importance, also contribute to the oxidation process. The unique properties of BSS, combined with the mechanical energy provided by ball-milling, can efficiently convert toluene to phenol in a single step, offering a more straightforward and resource-efficient alternative to traditional multi-step processes. The findings suggest potential applications for this method in industrial chemical synthesis, particularly in processes requiring the conversion of aromatic compounds. Moreover, the use of air as the oxidant and the absence of excessive oxidation makes this approach both environmentally friendly and economically viable.

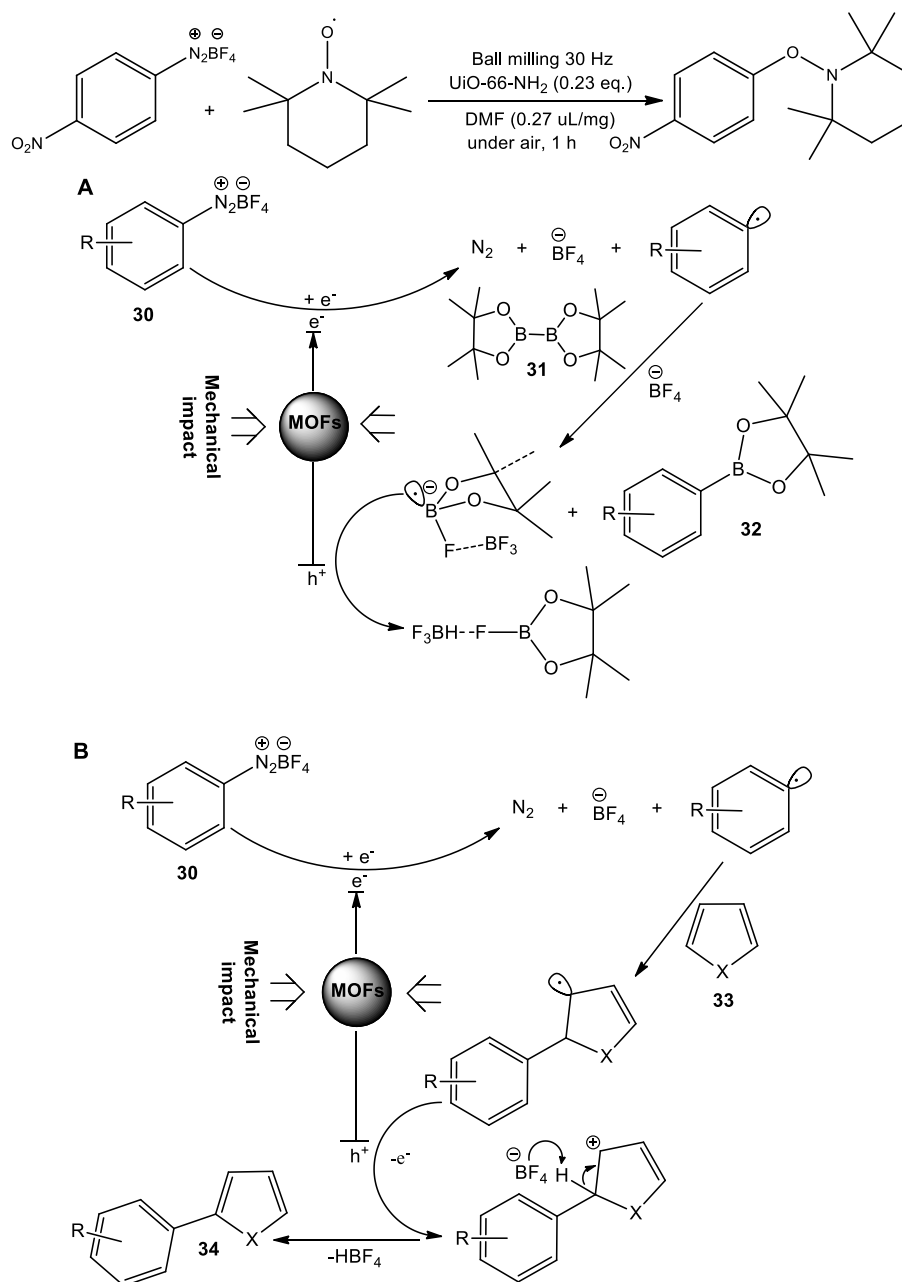


**Scheme 12.** Proposed mechanism of the oxidation of toluene to phenol.

In 2023, a piezochemically driven decarboxylative acylation of quinoxalin-2(1*H*)-ones **28** using ball milling, which utilizes BaTiO<sub>3</sub> as a piezoelectric material to convert mechanical energy into electrical potential, was reported (Scheme 13).<sup>32</sup> This piezoredox catalytic strategy, which does not require solvents and is carried out under mild conditions, leads to the efficient formation of C<sub>3</sub>-acylated quinoxalin-2(1*H*)-ones **29**. The optimal conditions were found by systematically varying reaction parameters, such as the type and amount of piezoelectric material, base, oxidant, and mechanical parameters like the size and number of milling balls. The piezoelectric properties of BaTiO<sub>3</sub> are critical for generating the required electrochemical potential to drive the reaction. BaTiO<sub>3</sub> particles of specific sizes (0.6-1 μm) yielded the best results, highlighting the importance of particle size on the piezoelectric effect. Comparisons with other materials, including non-piezoelectric and different piezoelectric materials, confirmed that BaTiO<sub>3</sub> had superior efficiency. The use of ball milling also resulted in a significant reduction in reaction time compared to conventional solution-phase methods, achieving yields up to 98% in as little as 18 min. Furthermore, the study explored the substrate scope, demonstrating broad applicability across various quinoxalin-2(1*H*)-one derivatives and α-oxocarboxylic acids, yielding products in good to excellent yields. Mechanistic studies suggested a radical pathway facilitated by the piezoelectric material under ball milling conditions. Control experiments confirmed the necessity of both the piezoelectric effect and the mechanical forces provided by the milling process. Equally importantly, the ability to conduct the reaction on a gram scale with high yield (95%) and recycle the piezoelectric material up to three times without significant loss of efficiency demonstrates the practical utility.



**Scheme 13.** General reaction and mechanism of the piezocatalyzed decarboxylative acylation of quinoxalin-2(1*H*)-ones.

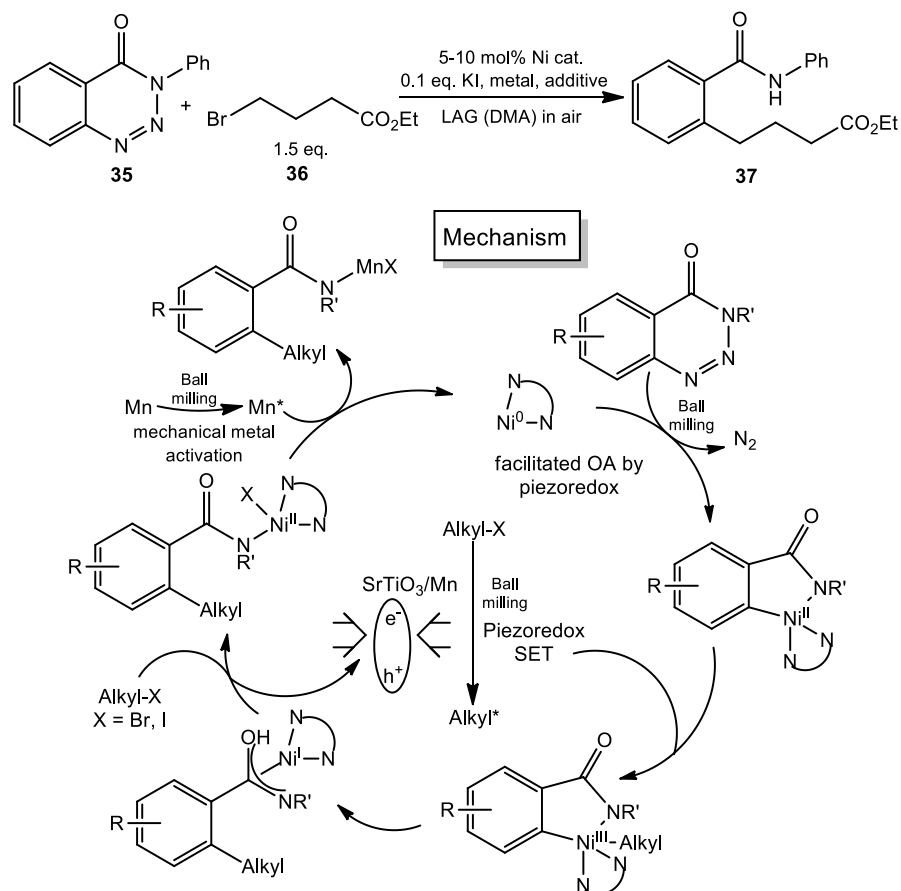


**Scheme 14.** General reaction and mechanisms of the mechanoredox reactions mediated by piezoelectric MOFs through ball milling: (A) borylation and (B) arylation.

Piezochemically driven borylation and arylation of benzenediazonium tetrafluoroborates **30** were later demonstrated using ball-milled metal-organic frameworks (MOFs) UiO-66 and UiO-66-NH<sub>2</sub> to yield borylated **32** and arylated products **34** (Scheme 14).<sup>33</sup> UiO-66-NH<sub>2</sub> demonstrated a lower N<sub>2</sub> adsorption capacity and Brunauer–Emmett–Teller (BET) surface area compared to UiO-66 due to the larger 2-aminoterephthalate ligand. Piezoresponse force microscopy (PFM) revealed that both MOFs exhibited piezoelectric properties, with UiO-66-NH<sub>2</sub> showing a higher piezoelectric coefficient ( $d_{33} = 62$  pm/V) than UiO-66 ( $d_{33} = 16$  pm/V). Both MOFs facilitated the formation of aryl radicals from aryl diazonium salts under ball milling conditions, subsequently reacting with bis(pinacolato)diborane **31** or heteroarenes **33**. The use of LAG additives significantly increased reaction yields, with DMF proving the most effective. UiO-66-NH<sub>2</sub> consistently outperformed UiO-66 due to its superior piezoelectric properties. Control experiments confirmed that the

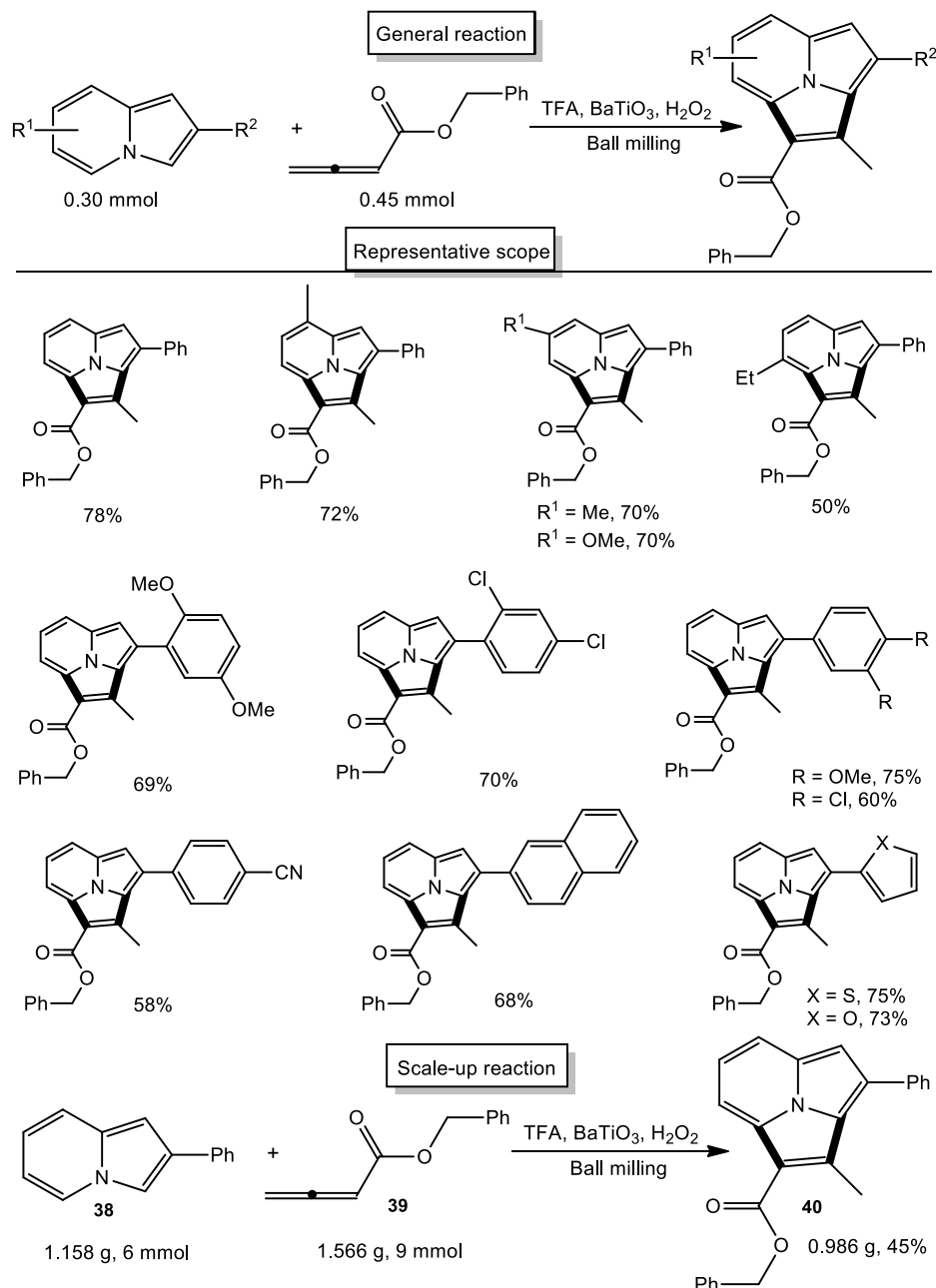
catalytic activity stemmed from the piezoelectric effect, as reactions without MOFs or with non-piezoelectric materials resulted in negligible yields. Tests varying milling frequencies showed reduced efficiency at lower frequencies, emphasizing the role of mechanical agitation in activating piezoelectricity. Importantly, the MOFs demonstrated excellent recyclability; after structural degradation from mechanical impact, the spent MOFs were regenerated using an acidic treatment, restoring their crystallinity and catalytic activity.

The Zou group reported a mechanoredox/Ni co-catalyzed method for cross-electrophile coupling of benzotriazinones with alkyl (pseudo)halides under air-tolerant, solvent-minimized conditions using ball-milling.<sup>34</sup> This approach utilizes Mn powders and piezoelectric materials like CaTiO<sub>3</sub>, SrTiO<sub>3</sub>, and BaTiO<sub>3</sub> under LAG conditions to enhance reactivity through radical generation via SET, eliminating the need for chemical activators. For example, the yields of product **37** from the reaction of 3-phenylbenzotriazinone **35** and ethyl 4-bromobutanoate **36** improved to 86–92% (Scheme 15), in contrast to a low yield observed in the control experiment using non-piezoelectric K<sub>2</sub>TiO<sub>3</sub>. SrTiO<sub>3</sub> demonstrated the highest effectiveness in enhancing efficiency. Interestingly, the carbonates (BaCO<sub>3</sub>, CaCO<sub>3</sub>, and SrCO<sub>3</sub>) also showed effectiveness, though to a lesser extent, possibly due to being converted into piezoelectric forms, such as oxides, during ball-milling. The method achieves high chemoselectivity for bromides over chlorides and enables efficient denitrogenative coupling with good to excellent yields across various substrates. Compared to conventional thermal catalysis, the reactivity of benzotriazinones is enhanced by piezocatalysis, while alkyl (pseudo)halides exhibit reduced reactivity under the mild conditions of LAG. As a result, the C<sub>Ar</sub>–Cl group in benzotriazinones is preserved, which is typically reactive in traditional methods. The use of SrTiO<sub>3</sub> facilitates the formation of alkyl radicals, complementing the single-electron reduction by Ni(I) species and enabling high yields despite the reduced reactivities. As also shown in **Scheme 15**, mechanistically, the activation of Mn powders removes the necessity for a chemical activator, while the highly efficient mixing process in ball milling minimizes the amount of DMA required as a solvent to just 1.0 μL mg<sup>−1</sup>, serving as a LAG. This process enhances the reactivity of the cyclic N-acyltriazene moiety in benzotriazinones to a level comparable to that of aryl bromides through ball-milling-induced mechanoredox. Consequently, this promotes the denitrogenative oxidative addition of Ni(0) to the C<sub>Ar</sub>–N3 bond at approximately room temperature. Additionally, the mechanoredox-generated alkyl radical from alkyl halides offsets the lower reactivity of alkyl halides under mild LAG conditions, ultimately achieving high chemoselectivity between alkyl/aryl bromides and chlorides.



**Scheme 15.** General reaction of the piezoredox/Ni co-catalyzed cross-electrophile coupling under LAG conditions using 3-phenylbenzotriazinone and ethyl 4-bromobutanoate. A plausible piezocatalytic cycle under LAG conditions is also shown.

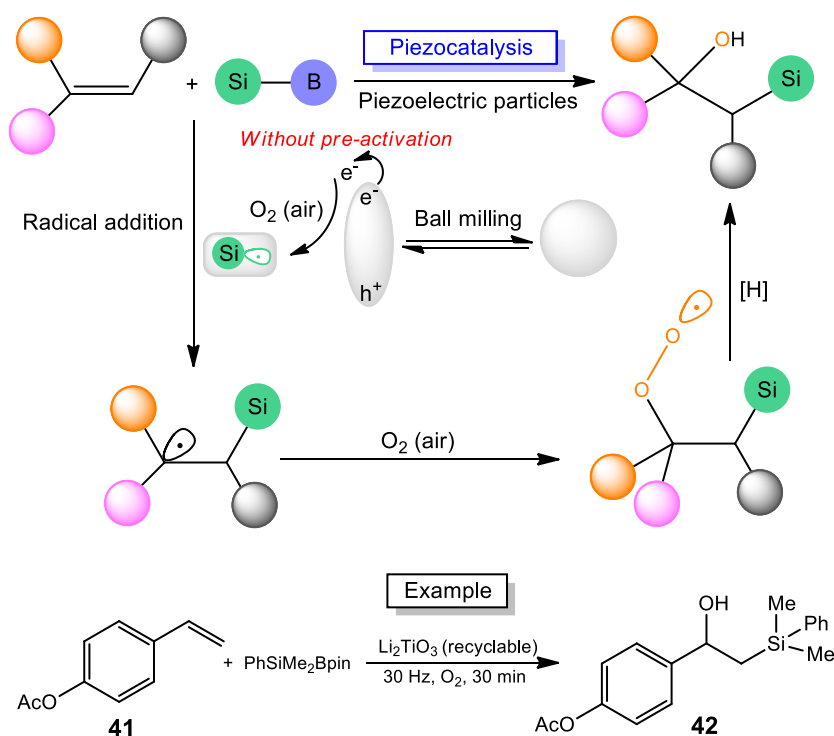
In 2024, the Cao group demonstrated a novel mechanochemical-induced method for synthesizing pyrrolo[2,1,5-*cd*]indolizine derivatives using indolizines and allenes in the presence of piezoelectric materials such as  $\text{BaTiO}_3$ ,  $\text{PbTiO}_3$ ,  $\text{LiNbO}_3$ , and  $\text{ZnO}$  under ball-milling conditions with LAG additives and oxidants (Scheme 16).<sup>35</sup> The use of cubic  $\text{BaTiO}_3$  as a charge-transfer catalyst significantly enhanced reaction efficiency, yielding a variety of derivatives with yields ranging from 50% to 82%, depending on the substrates. The optimized system showed consistent reactivity across various electron-donating and electron-withdrawing functional groups without compromising yield or regioselectivity. Mechanistic studies identified a free radical pathway driven by the temporary electrochemical potential generated by the piezoelectric material during ball milling. The mechanochemical [3 + 2] cyclization demonstrated scalability, as a scaled-up reaction using 1.158 g of 2-phenylindolizine **38** and 1.566 g of benzyl buta-2,3-dienoate **39** produced the desired product **40** with a yield of 45%. The proposed piezocatalytic route also achieves competitive yields compared to a photocatalytic route using rose bengal as a photosensitizer under 20 W blue LED, while being faster and more efficient.



**Scheme 16.** General reactions of indolizine carried out using 10 SS balls (4 × 10 mm Ø, 6 × 6 mm Ø), BaTiO<sub>3</sub> (<3 µm, 1.5 mmol), TFA (0.30 mmol), H<sub>2</sub>O<sub>2</sub> (30% in water, 0.60 mmol) in a 20 mL milling jar at 550 rounds per minute for 6 h. The isolated yields are shown as percentages. Scale-up reaction of the [3 + 2] cyclization of an indolizine with an allene, piezocatalytically driven by BaTiO<sub>3</sub>, is also shown here.

Lian and co-workers introduced a mechanochemical approach for 1,2-hydroxysilylation of alkenes,<sup>36</sup> an essential reaction in organic synthesis for producing important silicon-containing compounds. The use of piezoelectric materials such as BaTiO<sub>3</sub> under ball-milling conditions has been explored to facilitate SET reactions, offering a simpler and solvent-free synthetic methodology.<sup>23, 27</sup> Building on these foundational advancements, they investigated the potential of piezoelectric materials as redox catalysts for the 1,2-hydroxysilylation of alkenes via a SET pathway. The proposed reaction involves generating a silicon radical from silylboronate through oxygen activation and the transient polarization of a piezoelectric material, followed by adding radicals to alkenes. Using piezoelectric Li<sub>2</sub>TiO<sub>3</sub> particles as catalysts under ball-milling

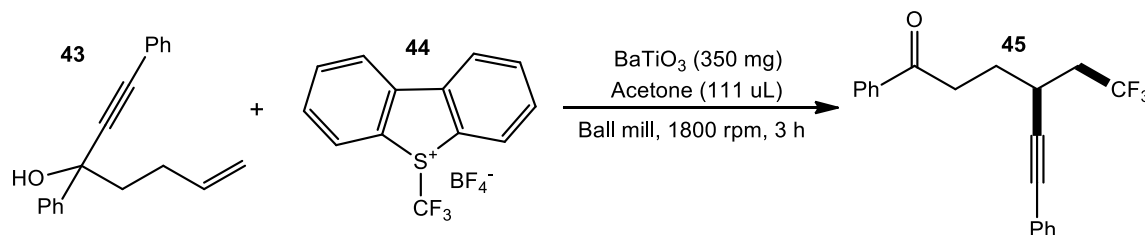
conditions, the process achieves efficient SET pathways to form silicon radicals. This method enables the reaction to proceed under mild, solvent-free conditions, with a rapid reaction time of 30 min. It successfully applies to both activated and unactivated alkenes, overcoming traditional challenges such as competing reactions. Substrate compatibility is broad, accommodating a range of functional groups, including those on pharmaceutical intermediates. The piezocatalyst is also reusable, maintaining activity after multiple cycles, and isotopic experiments identified oxygen gas and Bpin as sources of the hydroxyl oxygen and hydrogen atoms, respectively. The proposed method pioneers solid-liquid-gas triphasic reactions under ambient conditions and demonstrates potential for late-stage functionalization of complex molecules, including drugs and natural products. The mechanistic study revealed that the reaction proceeds via a radical pathway, utilizing the mechanical polarization of  $\text{Li}_2\text{TiO}_3$  to generate reactive species. The proposed synthesis protocol is environmentally friendly and scalable, showcasing advantages such as ease of operation, elimination of strong bases or external reductants, and applicability to various substrates. To confirm the scalability of the proposed method, the 1,2-hydroxysilylation of compound **41** was carried out at both 1 mmol and 2 mmol scales, producing the target product **42** with yields of 81% and 78%, respectively (Scheme 17). It is interesting to note the superior piezocatalytic activity of  $\text{Li}_2\text{TiO}_3$  compared to  $\text{K}_2\text{TiO}_3$ , which is piezocatalytically inactive for the cross-electrophile coupling of benzotriazinones with alkyl (pseudo)halides,<sup>34</sup> despite both possessing alkali metal cations.



**Scheme 17.** Scale-up reaction of the hydroxysilylation of an alkene.

Meanwhile, the Ouyang group explored piezoredox-enabled difunctionalization of unactivated alkenes via distal functional group migration, proposing an innovative mechanochemical approach that integrates piezoelectric material  $\text{BaTiO}_3$  with ball milling for radical-mediated carbotrifluoromethylation.<sup>37</sup> This method offers advantages, such as ease of handling, recyclable catalysts, air compatibility, and reduced solvent usage. It also demonstrates broad substrate applicability and has been proven to be robust through scaled-up experiments and catalyst recycling. The developed piezoredox strategy is the first to facilitate a multiple

cascade radical reaction, providing a rapid pathway to difunctionalized fluorine-containing ketone scaffolds. Umemoto's reagents and commercially available piezoelectric materials, including BaTiO<sub>3</sub>, LiNbO<sub>3</sub>, BaCO<sub>3</sub>, and ZnO, were tested in a GT300 grinding vessel to drive the reactions at room temperature under air. For example, substituted unactivated alkene **43**, Umemoto's reagent **44**, and BaTiO<sub>3</sub> (1.5 mmol, 5.0 eq.) were placed in a stainless-steel milling jar (5 mL) with two stainless-steel balls (7 mm in diameter) under air. Acetone (0.2  $\mu\text{L mg}^{-1}$ ) was added to the mixture, yielding 88% of the trifluoromethylated product **45**. BaTiO<sub>3</sub> was reused in subsequent reactions, and the yield of **45** was maintained at over 60% after five runs. The loss of BaTiO<sub>3</sub> during reuse was responsible for the decline in yield. A gram-scale reaction was also achieved, yielding 0.79 g of product **45** from 1.36 g of substrate **43**, with a recovery of 0.21 g of **43**.



**Scheme 18.** Piezocatalyzed difunctionalization of unactivated alkene.

Piezoredox-mediated polymerizations also offer opportunities to develop energy-efficient, environmentally friendly methods for synthesizing both commodity and novel polymers.<sup>7</sup> The Golder group has demonstrated the successful translation of piezocatalyzed polymerizations from sonication to ball milling, enabling high-molar-mass polymers with high monomer conversion in significantly shorter times (3 h vs. 8–21 h). The ball milling method avoids polymer degradation and can be performed in sealed jars prepared on the benchtop, unlike other mechanoredox polymerizations requiring inert environments. Under air, these reactions exhibit a 145-min induction period, hypothesized to result from oxygen reduction to superoxide, followed by complete monomer conversion within 5 min.

In 2023, Golder and co-workers reported the first piezoredox-catalyzed reversible addition–fragmentation chain transfer (RAFT) polymerization in a ball mill, using a trithiocarbonate chain transfer agent, diaryliodonium initiators and piezoelectric BaTiO<sub>3</sub>.<sup>38</sup> Mechanistic studies revealed that diaryliodonium reduction generates phenyl radicals to initiate polymer chains, with continuous milling essential for efficient mixing rather than redox processes (Figure 3). When BaTiO<sub>3</sub> is excluded from the reaction mixture, neither benzene nor iodobenzene are formed, showing the critical role of piezoredox processes in radical initiation. This approach offers advantages such as short reaction times, low energy consumption, and the ability to copolymerize traditionally immiscible monomers using LAG. While moderate conversion and higher dispersities were observed in ultrasound-assisted reactions due to chain scission and slow propagation, ball milling achieved high conversion in 3 h with low dispersities ( $\bar{M}_w/\bar{M}_n = 1.0\text{--}1.1$ ). Full conversion was demonstrated in 8 h using a benchtop vortexer, further enhancing accessibility. Energy studies revealed that ball milling and vortexing consume one-third the energy of traditional thermal RAFT methods. The method also enables the synthesis of block and random copolymers from chemically immiscible monomers (e.g., fluorinated and hydrophilic acrylates), overcoming challenges in conventional RAFT approaches.

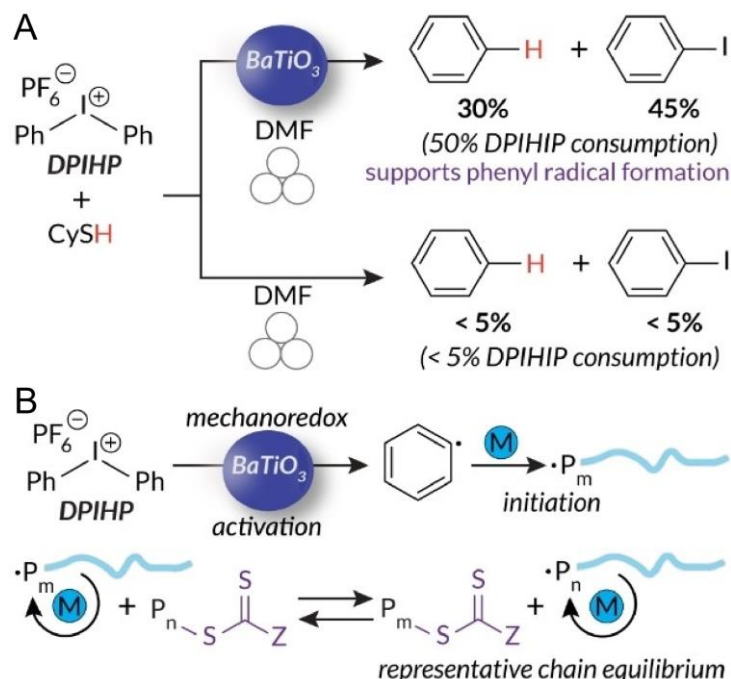


**Figure 3.** (A) Mechanistic studies of hydrogen atom transfer demonstrating the generation of phenyl radicals during piezoredox RAFT initiation with ball milling reactions conducted at 30 Hz for 3 h. (B) The proposed RAFT mechanism based upon small molecule studies. DPIHP denotes diphenyl iodonium hexafluorophosphate. Reproduced from Ref. 38 with permission. Copyright 2023 Wiley-VCH GmbH.

## 5. Piezocatalyzed Organic Transformations under Mixing

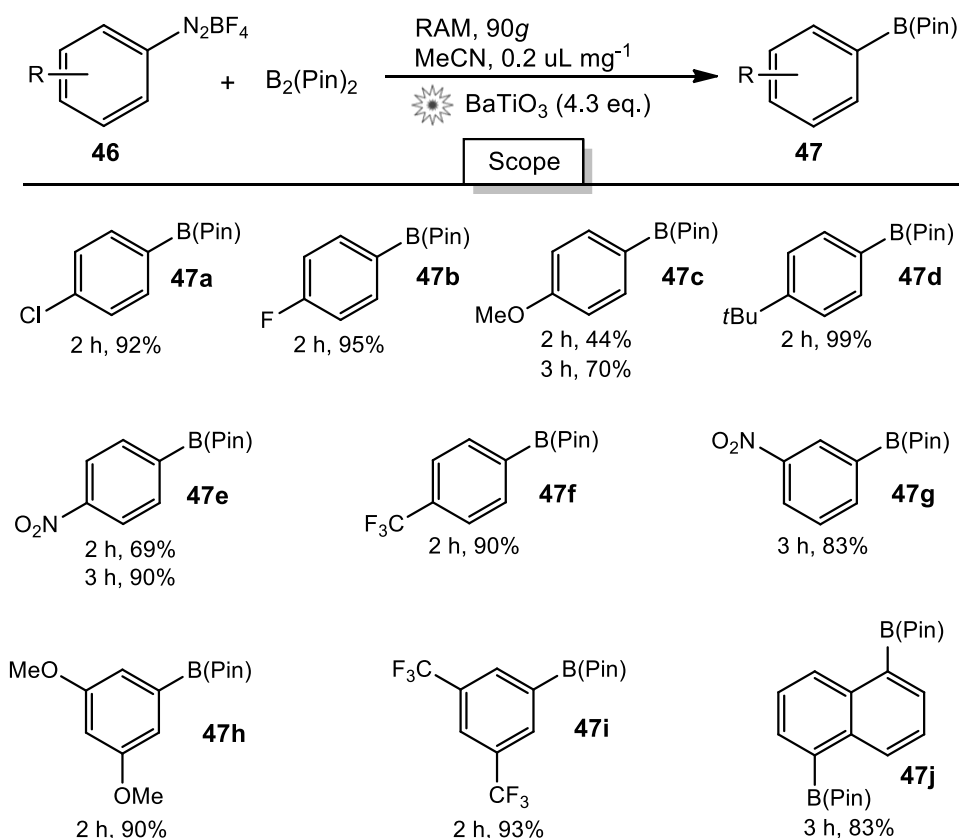
To enable mixing and blending of reactants without the need for bulk solvent or milling media, facilitating piezocatalyzed reactions, one can use resonant acoustic mixing (RAM). RAM uses low-frequency acoustic energy to induce rapid and uniform mixing of powders, pastes, and other materials.<sup>39</sup> Unlike traditional ball milling, which relies on mechanical grinding and impact, RAM operates by transferring vibrational energy into a container, creating a fluidized mixing environment. Mechanochemistry traditionally relies on impact and mixing resulting from the use of balls or screws, but RAM has recently emerged as a strategy to conduct mechanochemical reactions without such milling or crushing media. Instead, RAM achieves reactivity by shaking materials at a low acoustic frequency (e.g., 60 Hz), with energy input modulated through changes in the vertical acceleration of the reaction vessel.<sup>40</sup> This allows for efficient blending of materials at a molecular level without the need for moving parts inside the mixing vessel, reducing localized overheating or degradation of reactive materials.

Compared to traditional ball milling, RAM offers several advantages, including faster processing times, reduced contamination (since there are no milling media), and the ability to mix highly viscous or sensitive materials without excessive wear.<sup>39</sup> By avoiding the need for milling media, RAM enables simplification of reaction design, eliminates product contamination resulting from chipping and abrasion, and facilitates scale-up. Additionally, it can support solvent-free reactions, making it an environmentally friendly alternative. However, RAM also has disadvantages, such as higher initial costs and limitations in controlling particle size reduction, as it primarily focuses on mixing rather than grinding.<sup>39</sup> In contrast, ball milling provides greater control over particle size but suffers from longer processing times and potential contamination from milling

media. Thus, RAM is particularly relevant for mechanochemical synthesis when uniform mixing, reaction efficiency, and scalability are priorities over fine particle size control.

In organic synthesis, RAM has been employed for metal-catalyzed coupling reactions by the Friščić group.<sup>41, 42</sup> Unlike ball milling, RAM simplifies reaction design by eliminating the need for grinding media, while also enabling easier scalability.<sup>42</sup> They later demonstrate that, even without mechanical impact from milling media, RAM supports piezoredox catalysis.<sup>40</sup> Using commercial cubic BaTiO<sub>3</sub> as a catalyst, SET borylation and arylation of diazonium salts can be achieved (Scheme 19), successfully scaling the reaction from approximately 0.1 grams to at least gram-scale quantities.

The borylation of aryldiazonium salts was initially tested using p-chlorobenzenediazonium tetrafluoroborate **46a** and bis(pinacolato)boron (bpb) as substrates.<sup>40</sup> Acoustic mixing was conducted with a Resodyn LabRAM II, placing samples in glass vials mounted on custom holders. RAM of an equimolar 0.3 mmol mixture of **46a** and bpb at an acceleration of 90g ( $g = 9.81 \text{ m s}^{-2}$ ) yielded no reaction. However, adding 300 mg (4.3 eq.) of BaTiO<sub>3</sub> resulted in ~10% conversion to product **47a** after 3 h. Similar yields were observed with small amounts of non-polar liquid additives, such as hexanes (17%) or toluene (13%). Here, it is obvious that piezoelectric materials are a prerequisite for these RAM-piezocatalyzed organic transformations. Using acetonitrile significantly improved conversion to 92% in 3 h, matching the efficiency of ball-milling under similar conditions.<sup>23</sup> Under these optimized RAM conditions, a variety of aryldiazonium salts with diverse aromatic ring substituents reacted efficiently. Most substrates achieved high ( $\geq 80\%$ ) to excellent ( $\geq 95\%$ ) yields within 2 h. For those with initially lower conversions (e.g., substrates **46c**, **46d**), extending the reaction time to 3 h significantly improved yields (e.g., **47d** increased from 69% to 90%). NMR yields for substrates **46a–46g** (70–99%) were notably higher than those reported for ball-milling (52–86%). No clear trend was observed between electronic effects and reaction efficiency, as both electron-donating (–OMe, **46h**) and electron-withdrawing (–CF<sub>3</sub>, **47i**) substituents yielded over 90% conversion after 2 h. RAM's efficiency also enabled access to ditopic substrates, such as **46j**, which afforded **47j** in 92% yield (96% per boron function, 67% isolated yield) using 2.1 equivalents of bpb. The RAM reaction mechanism appears similar to ball-milling, proceeding via a radical SET pathway.



**Scheme 19.** NMR yields of products with various substituents. Reaction conditions: 0.3 mmol **46a–46j**, 0.3 mmol bpb (0.63 mmol for **46j**), 1.29 mmol (4.3 equivalents) of  $\text{BaTiO}_3$ , acetonitrile ( $\eta = 0.25 \text{ mL mg}^{-1}$ ) under RAM acceleration of 90g for 2 or 3 h.

Overall, the proof-of-concept studies demonstrate that the activation of piezoelectric materials is initiated by external mechanical stress, such as sonication or mechanical vibration through milling. This process generates transient polarization, resulting in the formation of opposite charges (electron and hole) that can drive chemical reactions. This stress-induced polarization allows the strained piezoelectric materials to act as electron donors or acceptors in redox reactions. Piezoelectric materials can facilitate SET, generating radicals or other reactive species that drive organic transformations. Piezoelectric materials can activate C-H bonds, enabling functionalization reactions such as arylation, borylation, and trifluoromethylation and drive decarboxylative coupling reactions, leading to the formation of carbonyl compounds. Polymerization reactions can also be driven piezocatalytically.

Piezocatalyzed organic transformations with ball milling offer at least two advantages. First, these reactions can be performed with little or no solvent, making them more environmentally friendly. Secondly, the scalability of reactions has been demonstrated by successful gram-scale syntheses. It is hypothesized that piezoelectric materials allow for selective activation of specific bonds or functional groups, enhancing reaction specificity due to their uniquely strained surfaces. In the case of piezocatalyzed organic transformations with ultrasound vibration, it has been proven to broaden the reaction scope and drive redox reactions relevant to polymer chemistry that are otherwise inaccessible with conventional methods. Meanwhile, mixing with resonance acoustics provides faster reaction times and higher yields than ball milling.

## 6. SET as a Fundamental Process in Piezocatalyzed Organic Synthesis

SET is a fundamental process in piezocatalysis, facilitating radical generation, bond activation, and functional group transformations. The feasibility of a SET reaction is determined by the redox potential of the involved species, which dictates whether electron donation (reduction) or electron acceptance (oxidation) is thermodynamically viable. Redox potentials provide a quantitative measure of a molecule's ability to accept or donate electrons, influencing the efficiency and selectivity of SET-based transformations. Typically, the redox potentials for organic substrates fall within the range of  $-2.5$  V to  $+2.5$  V vs. normal hydrogen electrode (NHE),<sup>43</sup> where reduction reactions generally require highly negative potentials, and oxidation reactions demand positive ones.

To evaluate redox potentials in organic reactions, electrochemical and spectroscopic techniques can be utilized. Cyclic voltammetry provides information about the redox behavior of molecules by measuring current as a function of applied voltage.<sup>44</sup> This method helps determine the oxidation and reduction potentials of organic compounds and catalyst materials by analyzing peak positions and reversibility of redox events. Differential pulse voltammetry and square wave voltammetry offer higher sensitivity than cyclic voltammetry,<sup>45</sup> allowing precise determination of redox potentials, particularly for low-concentration species. Differential pulse voltammetry is often used to distinguish closely spaced redox events, making it valuable for assessing complex reaction mixtures. Meanwhile, electrochemical impedance spectroscopy provides insight into the charge transfer kinetics and interfacial resistance of redox-active species, which is particularly useful for understanding electron transfer dynamics.<sup>46</sup> On the other hand, spectroelectrochemistry, which combines electrochemical methods with UV-Vis, IR, or EPR (electron paramagnetic resonance) spectroscopy, enables real-time monitoring of redox processes, helping to identify intermediates and reaction pathways.<sup>47</sup> Computational methods, such as DFT calculations, are frequently employed to predict redox potentials by modeling electron density distribution and energy levels of molecular orbitals.<sup>48</sup> In particular, computational methods provide a low-cost and straightforward approach to estimating the required redox potentials necessary for SET reactions between the piezoelectric material and the reactant being activated. Therefore, the types of transformations that can be achieved using a given piezoelectric material can be predicted.

On the reductive side, for example, aryl halides undergo SET to generate aryl radicals, which subsequently participate in cross-coupling or radical addition reactions.<sup>49</sup> The reduction potential for this transformation depends on the halide substituent, following the trend  $I > Br > Cl$ , with potentials typically ranging from  $-1.5$  V to  $-2.5$  V vs. NHE. The generation of aryl radicals via reductive SET plays a key role in metal-free arylation reactions and radical-mediated polymerizations.<sup>50</sup> Similarly, ketones and aldehydes can be reduced to ketyl radicals at potentials between  $-1.5$  V and  $-2.0$  V vs. NHE,<sup>51</sup> forming reactive intermediates essential in pinacol coupling, benzoin condensation, and electroreductive carbonyl functionalization. Another important reductive SET process is the one-electron reduction of  $CO_2$  to its radical anion, which occurs at approximately  $-1.9$  V vs. NHE.<sup>51, 52</sup> This transformation is a crucial step in  $CO_2$  utilization strategies, such as electrocatalytic and photocatalytic  $CO_2$  reduction.

Oxidative SET reactions, on the contrary, involve the transfer of an electron from an organic substrate to an oxidizing species. For instance, the oxidation of benzyl alcohol to its radical cation occurs at potentials ranging from  $+1.5$  V to  $+2.0$  V vs. NHE,<sup>53</sup> facilitating subsequent transformations such as aldehyde formation and radical polymerization. Similarly, arylamines can be oxidized to aminium radicals at  $+0.7$  V to  $+1.5$  V vs. NHE, playing a significant role in oxidative coupling reactions and conductive polymer synthesis.<sup>54</sup> More demanding oxidation processes, such as C–H activation in hydrocarbons, typically require potentials above

+1.8 V to +2.5 V vs. NHE,<sup>55</sup> making them challenging to achieve under mild reaction conditions without strong oxidants.

Typical oxidation potential ranges for organic functional groups, redox mediators, and solvents are depicted in Figure 4.<sup>56</sup> The values are referenced against the saturated calomel electrode (SCE). The potential of the SCE is +0.244 V relative to NHE. Therefore, to convert a potential measured against SCE to NHE, we need to add 0.244 V to the value measured against SCE. For example, if the potential vs. SCE is +0.5 V, the corresponding potential vs. NHE would be +0.744 V.

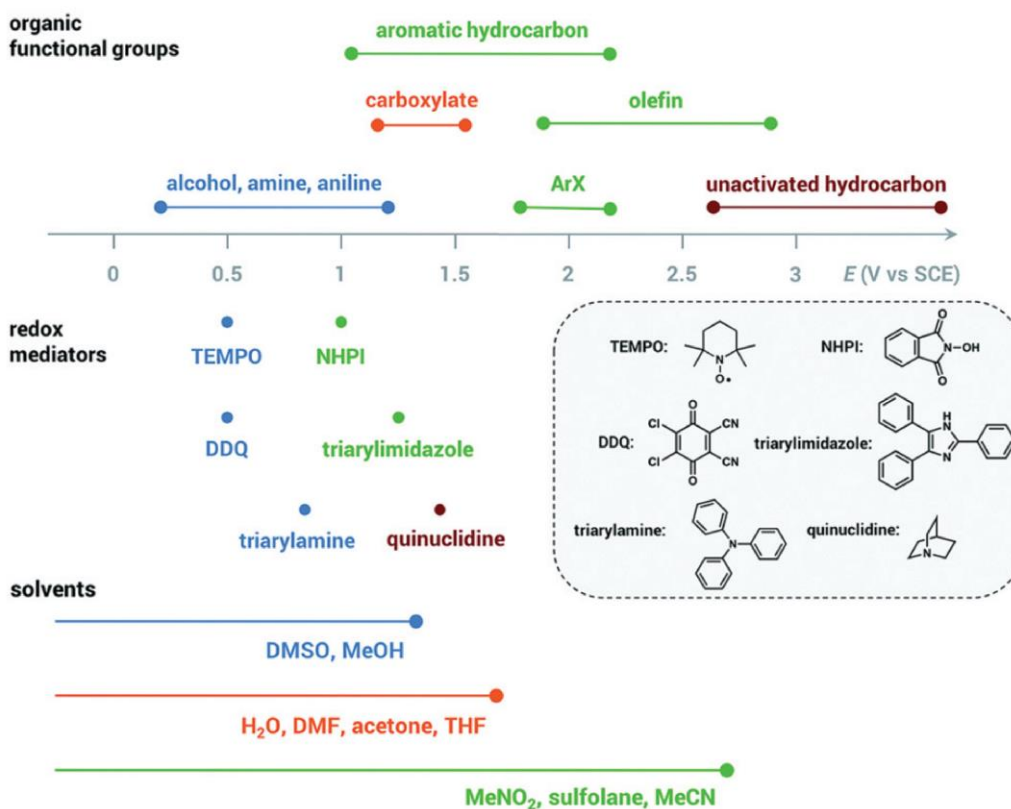


**Figure 4.** The oxidation potentials of some organic functional groups, redox mediators, and solvents. Reproduced from Ref. 56 with permission. Copyright 2020 Royal Society of Chemistry.

Piezoelectric materials such as ZnO, BaTiO<sub>3</sub>, and PZT generate localized electrostatic potentials upon mechanical stress, typically in the range of  $\pm 1$  to  $\pm 2$  V.<sup>57, 58</sup> This ability suggests that they could effectively mediate specific SET reactions in organic synthesis by acting as dynamic electron donors or acceptors. For example, negative piezopotentials around -1.5 V could enable the reduction of aryl halides, facilitating radical-driven cross-coupling and polymerization reactions. Similarly, the reduction of ketones to ketyl radicals may be achievable at sufficiently high negative potentials, making piezoelectric materials attractive candidates for electrochemical pinacol coupling. Furthermore, the mechanochemically induced reduction of CO<sub>2</sub> could be possible if the local piezopotential approaches -1.9 V, potentially offering a sustainable approach to CO<sub>2</sub> valorization without external electrical bias. Conversely, positive piezopotentials around +1.5 V may drive oxidative SET reactions, such as the oxidation of benzyl alcohols or arylamines, facilitating aldehyde synthesis or amine coupling reactions. While many oxidative SET processes require higher potentials above +2 V, coupling piezoelectric effects with co-catalysts or applied strain modulation may extend the range of accessible transformations. In redox catalysis, co-catalysts, usually composed of noble metals like Pt, Au, and

Pd, play a crucial role in lowering the activation barrier by providing additional active sites and facilitating electron transfer. Their unique electronic structures and high conductivity enhance charge separation and promote efficient interaction between the catalyst and reactants, thereby reducing energy requirements for bond activation. Additionally, noble metal co-catalysts can tune the tendency of SET reactions by modifying the work function of the catalytic system. By altering the electronic properties of the primary catalyst (the piezoelectric material), they influence the energy alignment between the catalyst and the reactant, optimizing electron flow and selectivity. This fine-tuning enables precise control over reaction pathways, improving efficiency and selectivity in redox transformations.

Undoubtedly, redox potentials must be carefully considered when selecting an appropriate piezoelectric material for redox transformations. This requires a thorough evaluation of its piezopotential range and how well it aligns with the redox potentials of the desired SET reactions. The key factors include intrinsic piezoelectric potential, as different materials generate distinct piezopotentials under mechanical stress. For example, BaTiO<sub>3</sub> and PZT can generate potentials in the range of  $\pm 1.5$  to  $\pm 2$  V, making them suitable for moderate redox reactions, while ZnO typically generates lower potentials ( $\sim \pm 1$  V), which may be useful for milder transformations. The band structure and work function of a piezoelectric material dictate its ability to participate in SET reactions. If the CB edge bottom is positioned lower than the reduction potential of a given substrate, electron transfer is unlikely. Conversely, if the VB edge top is too high compared to the oxidation potential of a reactant, oxidation may not proceed. Dielectric and ferroelectric properties also play a role, as materials with high dielectric constants and ferroelectric behavior, such as PZT, tend to exhibit stronger and more sustained piezopotentials under mechanical stress. This can enhance SET reaction efficiency, particularly for challenging transformations that require extended charge separation. Surface functionalization and composite strategies could enhance charge transfer efficiency. Hybrid materials that combine piezoelectric properties with conductive components could also improve SET efficiency by facilitating charge transfer, for example, by coupling BaTiO<sub>3</sub> with a conductive carbon matrix. Tailoring piezoelectric material properties through doping strategies, composite (heterojunction) structures, and strain engineering to optimize their redox compatibility with specific SET transformations is an important topic for future research. The interplay between piezoelectric potential dynamics, interfacial charge transfer, and reaction kinetics needs to be well-understood.

Stability in reaction media is another critical factor. Some piezoelectric materials degrade in solution or lose piezoelectric activity over time. For example, BaTiO<sub>3</sub> can undergo hydrolysis in aqueous media,<sup>59</sup> whereas ZnO may dissolve under acidic conditions.<sup>60</sup> Thus, the selection should take into account the chemical stability of the material in the reaction medium. How to select potentially efficient piezocatalysts is discussed in more detail in the subsequent section.

## 7. Selecting Potentially Efficient Piezocatalysts

Thus far, BaTiO<sub>3</sub> is the most commonly used piezoelectric material for organic transformations, including Cu-catalyzed ATRC, C–H decarbonylation, arylation, and trifluoromethylation, achieving yields ranging from 62% to 99%.<sup>1, 6</sup> BaTiO<sub>3</sub> is also almost always used in piezocatalyzed polymerization. Following BaTiO<sub>3</sub>, ZnO is the second most utilized piezoelectric material, particularly in Cu-catalyzed ATRC and radical polymerization, with yields ranging from 80% to 92%, although it is completely inactive for other reactions such as C–H decarbonylation. LiNbO<sub>3</sub> has also demonstrated effectiveness in arylation and trifluoromethylation, giving yields of up to 43%. Equally importantly, SrTiO<sub>3</sub> has shown promise as a piezocatalyst for Cu-catalyzed ATRC,

achieving yields of up to 50%. SrTiO<sub>3</sub> itself is known as a highly active catalyst for heterogeneous photoredox H<sub>2</sub> production via water splitting when appropriately loaded with rhodium and cobalt co-catalysts.<sup>61</sup>

There are numerous opportunities to engineer perovskite-structured titanates, such as BaTiO<sub>3</sub> and SrTiO<sub>3</sub>, as well as niobates such as LiNbO<sub>3</sub>, through approaches like metal doping, to enhance and tune their piezocatalytic performance. Other piezoelectric materials, not necessarily limited to perovskite-structured oxides, could also potentially be used to drive redox reactions. Selecting suitable piezoelectric materials involves evaluating several key factors to ensure that the material not only converts mechanical energy into electrical energy but also drives chemical reactions. In general, piezoelectric materials that are sensitive to low-frequency mechanical energy are preferred, as they can more efficiently convert mechanical energy into electrical energy. However, readers should be aware that piezoelectric materials with this characteristic are not necessarily piezocatalytically active, as their surfaces must also efficiently drive the desired reactions and facilitate the selective transformation of reactants into the target products. A good piezoelectric material is not always a good piezocatalyst. Key considerations when selecting piezoelectric materials are as follows:

- (1) Stress constant. The stress constant measures the ability of a material to generate an electric charge in response to mechanical stress. A higher stress constant indicates a greater capacity to convert mechanical energy into electrical energy,<sup>62</sup> thereby potentially enhancing catalytic efficiency by providing a stronger driving force for charge transfer reactions. Materials with high piezoelectric constants, such as PZT, BaTiO<sub>3</sub>, and certain polymers like polyvinylidene fluoride (PVDF), are good options for piezocatalyzed chemical reactions because they can generate large electric fields under mild mechanical forces.
- (2) Coupling coefficient. Unlike the stress constant, which focuses on the magnitude of charge or strain produced and is an intrinsic material property, the coupling coefficient emphasizes the efficiency of energy conversion and depends on a combination of the properties of the material and device geometry.<sup>63</sup> Note that although the terms "constant" and "coefficient" refer to distinct concepts—a constant being a fixed, unchanging value, and a coefficient serving as a multiplier for a variable—these terms are often used interchangeably in piezocatalysis studies.
- (3) Curie temperature. The Curie temperature is the temperature at which certain materials undergo a phase transition, resulting in a change in their magnetic or electric properties. For piezoelectric materials, the Curie temperature is the point at which the material loses its piezoelectric properties because it transitions from a ferroelectric (polarized) state to a paraelectric (non-polarized) state.<sup>64</sup> A high Curie temperature allows the piezoelectric effect to remain functional across a wider temperature range. This property is important in piezocatalysis, as mechanical impacts within the jar during milling and the collapse of cavitation bubbles during sonication generate heat, thereby increasing the temperature of the reaction mixture.
- (4) Stability and durability. The material should withstand the operational environment, including exposure to reactants and solvents. Materials that are chemically stable and resistant to corrosion are ideal. In contrast, materials that degrade or lose their piezoelectric properties under reaction conditions are less desirable. The longevity of the piezoelectric material is particularly important for industrial applications where continuous or repeated use is required.<sup>65</sup>
- (5) Electrical and thermal conductivity. Good electrical conductivity facilitates the transfer of generated charges to catalytic sites.<sup>66</sup> Meanwhile, high thermal conductivity aids in dissipating the heat generated during the catalytic reaction, preserving its piezoelectric properties by keeping its temperature well below the Curie temperature.
- (6) Mechanical properties, such as toughness, flexibility, and brittleness. For catalysis driven by mechanical forces, the material must withstand repetitive mechanical stress, maintaining a strained structure without

cracking. Materials that are too brittle may fracture under stress,<sup>67</sup> leading to reduced catalytic activity and a shorter lifespan. In contrast, materials with good mechanical flexibility can better withstand repeated mechanical deformation, making them more suitable for applications involving dynamic mechanical loading.

- (7) Surface area and porosity. A high surface area allows more active sites to be available for catalytic reactions, typically increasing the overall reaction rate. A high density of active sites, specific to a particular substrate, per unit surface area is also essential for enhancing product selectivity. Meanwhile, porous piezoelectric materials can provide greater surface exposure to reactants and facilitate mass transport when involving solvents. Materials such as porous ceramics or nanostructured piezoelectric composites typically offer high surface areas, which can be beneficial for catalysis, especially in piezocatalytic reactions carried out in solution using ultrasound, where mass transfer limitations can be a significant factor.
- (8) Density of bulk and surface defects. Modulating defect density in the bulk can potentially increase the concentration of charge carriers by utilizing unpaired charges at defect sites.<sup>68</sup> Careful tuning of surface defects is also important for improving substrate binding and activation efficiency to satisfy the Sabatier principle. The Sabatier Principle suggests that for a catalyst to be effective, the interaction between the catalyst and the reactant must strike a balance: it should be strong enough for reactants to adsorb and undergo reaction but weak enough to allow the products to desorb.<sup>69</sup> If the interaction is too weak, the reaction cannot proceed efficiently, and if too strong, intermediates or products remain bound, inhibiting activity. The Sabatier Principle is particularly relevant for piezocatalytic reactions conducted in solution under ultrasound irradiation. In such systems, achieving the optimal balance of interaction strength between the catalyst and reactants is crucial to enhance catalytic activity, as the mechanical forces and ultrasonic energy can influence the adsorption, reaction, and desorption on the catalyst surface.
- (9) Particle dimension (size) and morphology (shape). The dimension and morphology of piezoelectric materials should be carefully designed, as they influence piezoelectric and catalytic behavior. The effects of particle dimension from 0D to 3D that are beneficial to piezoelectricity<sup>70-73</sup> and potentially relevant to catalysis can vary as follows:
  - 0D: Generates localized electric potential differences with limited deformation scalability.
  - 1D: Offers stronger directional deformation and enhanced charge migration.
  - 2D: Provides high flexibility, efficient charge distribution, and large-area deformation.
  - 3D: Maximizes force capture and charge collection efficiency through complex architectures
 Different morphologies (shape, structure, and surface characteristics) also have distinct effects on piezoelectric properties as follows:
  - Nanoparticles: Spherical particles distribute stress uniformly, resulting in isotropic piezoelectric responses. Larger nanoparticles generate stronger local electric fields, but their deformation is minimal compared to elongated structures.<sup>74</sup>
  - Nanorods/Nanowires: Elongated structures promote anisotropic deformation, where stress along the length generates large polarization.<sup>75</sup> The curvature effect amplifies charge separation and facilitates charge migration.<sup>76</sup> Charge separation and then migration to surface active sites are keys to achieving efficient performance in heterogeneous charge-carrier-based catalysis.
  - Nanosheets: Flat, thin structures with large surface areas deform more efficiently under mechanical forces.<sup>77</sup> Charge separation and distribution may also be improved due to the wide planar surface.
  - Hierarchical structures: Complex, branched architectures effectively capture stress from multiple directions. Mechanical coupling and charge collection efficiency can be maximized, enhancing overall

piezoelectric output.<sup>78</sup> Porous structures can also allow simultaneous mechanical deformation and charge transport.

- (10) Particle agglomeration and aggregation. Minimizing particle agglomeration (a reversible process) and aggregation (a typically irreversible process) is important to prevent the absorption of mechanical energy by strongly attached particles during their detachment,<sup>79</sup> especially when using ultrasound, as this could reduce the acoustic intensity available for the reaction.
- (11) Environmental and economic considerations. The chosen material should be readily available, cost-effective, and environmentally benign. While materials like lead-based piezoelectrics (e.g., PZT) offer high piezoelectric coefficients, they raise concerns due to their toxicity and environmental impact. Toxicity concerns are particularly important in the pharmaceutical industry. Alternatives such as lead-free piezoelectric ceramics (e.g., bismuth sodium titanate, BNT) or organic piezoelectric materials (e.g., PVDF) provide better options.
- (12) The compatibility with the catalytic process and the specific application requirements. The piezoelectric material should be chosen based on the type of catalytic reaction, the operating conditions, and the desired products. For instance, the yield of the desired products shifts from  $\alpha$ -arylacylamides to oxindoles even when using the same precursor,  $\alpha$ -bromo N-sulfonyl amides, by changing the piezoelectric material from BaTiO<sub>3</sub> and PbTiO<sub>3</sub>.<sup>28</sup>

Notably, selecting piezoelectric materials appropriate for catalysis involves a careful assessment of their piezoelectric properties, stability, conductivity, mechanical strength, surface characteristics, environmental impact, and compatibility with the intended application. By considering these factors, one can opt the most suitable piezoelectric materials to drive a specific catalytic reaction selectively, rapidly, and stably toward the desired product. The performance metrics to be considered when evaluating piezoelectric materials are summarized in Table 1. For a piezoelectric material to qualify as a good piezocatalyst, it should meet most of the metrics outlined in Table 2.

Once potential materials are identified and satisfy most of the parameters listed in Table 1, further evaluation is required using the metrics outlined in Table 2. If these evaluations are successful, highly efficient piezocatalysts may be obtained. However, even in such cases, this represents only a laboratory-scale achievement. To progress toward real-setting applications, several research tasks must be undertaken, as outlined in Figure 5. Using the information from Table 1 and Table 2, potential materials for specific piezocatalytic applications and modification strategies can be designed. At a minimum, three key aspects must be considered during catalyst design: (i) energy band alignment (for semiconducting piezocatalysts), (ii) charge carrier migration, and (iii) surface reaction selectivity. After candidate materials are synthesized, they will undergo structural characterization and evaluation of their piezocatalytic behavior, ideally using in-situ and operando techniques. Theoretical studies, such as those employing machine learning (ML), can accelerate catalyst design through cross-correlation and reciprocal feedback. All these tasks are iterative processes that require substantial investment in research. Once piezocatalysts with the best performance are identified, they must be integrated into an appropriate reactor. The reactor should be designed based on factors like the physicochemical properties of the piezocatalyst, process requirements, and economic constraints.

**Table 1.** Performance metrics of piezoelectric materials relevant to catalysis

Parameter	Definition	Units	Importance
Stress constant ( $e_{ij}$ )	Charge generated per unit stress applied.	C m <sup>-2</sup>	Reflects the efficiency of converting mechanical energy into electrical energy.
Coupling coefficient ( $k_{ij}$ )	Efficiency of energy conversion between mechanical and electrical forms.	Dimensionless	Higher values indicate better energy conversion efficiency.
Dielectric constant ( $\epsilon_r$ )	Ability to store electrical energy in the presence of an electric field.	Dimensionless	Affects the efficiency and energy density of piezoelectric materials.
Mechanical quality factor ( $Q_m$ )	Efficiency of mechanical energy transfer within the material.	Dimensionless	Indicates energy losses during mechanical vibrations.
Curie temperature ( $T_c$ )	Maximum temperature at which the material retains piezoelectric properties.	°C or K	Important for catalytic reactions that are sensitive to temperature.
Elastic compliance ( $S_{ij}$ )	Measure of material deformation under mechanical stress.	m <sup>2</sup> N <sup>-1</sup>	Determines how easily the material responds to stress.
Coercive field ( $E_c$ )	Minimum electric field required to depolarize the material.	kV cm <sup>-1</sup>	Indicates the resilience of the material to electrical bias.

**Table 2.** Performance metrics of catalytic materials relevant to piezocatalysis

Parameter	Definition	Measurement	Units	Importance
Activity	Ability to speed up a chemical reaction.	Reaction rate; Turnover Frequency (TOF): the number of reactions completed per active site per unit of time.	$\text{mol s}^{-1}$ ; $\text{s}^{-1}$	Determines how efficiently the catalyst accelerates the reaction under given conditions.
Selectivity	Ability to favor the formation of a specific product.	Fraction; Percentage of desired product in the total product mixture.	%	Reduces byproducts, improves process efficiency, and lowers purification costs.
Productivity	How effectively a catalyst facilitates the formation of desired products during a given time.	Space-Time Yield (STY): the amount of product formed per unit of catalyst or unit volume of reactor per unit of time.	$\text{mol g}^{-1} \text{ h}^{-1}$ ; $\text{mol m}^{-3} \text{ h}^{-1}$	Measures overall efficiency of the catalyst in producing the target product.
Stability	How well a catalyst maintains its performance (activity, selectivity, or structural integrity) over time.	Turnover Number (TON): the total number of products per active site before the catalyst deactivates; deactivation rate; half-life.	Dimensionless; $\text{mol g}^{-1} \text{ h}^{-1}$ ; $\text{h}^{-1}$	Ensures long-term reliability and reduces operational costs through minimal replacement needs.
Charge efficiency	How efficiently the produced charges are utilized to drive a chemical reaction.	The ratio of the number of reaction events (e.g., moles of product) to the number of electric charges generated by the catalyst on mechanical activation.	%	Represents charge utilization efficiency like quantum efficiency in photocatalysis or Faradaic efficiency in electrocatalysis

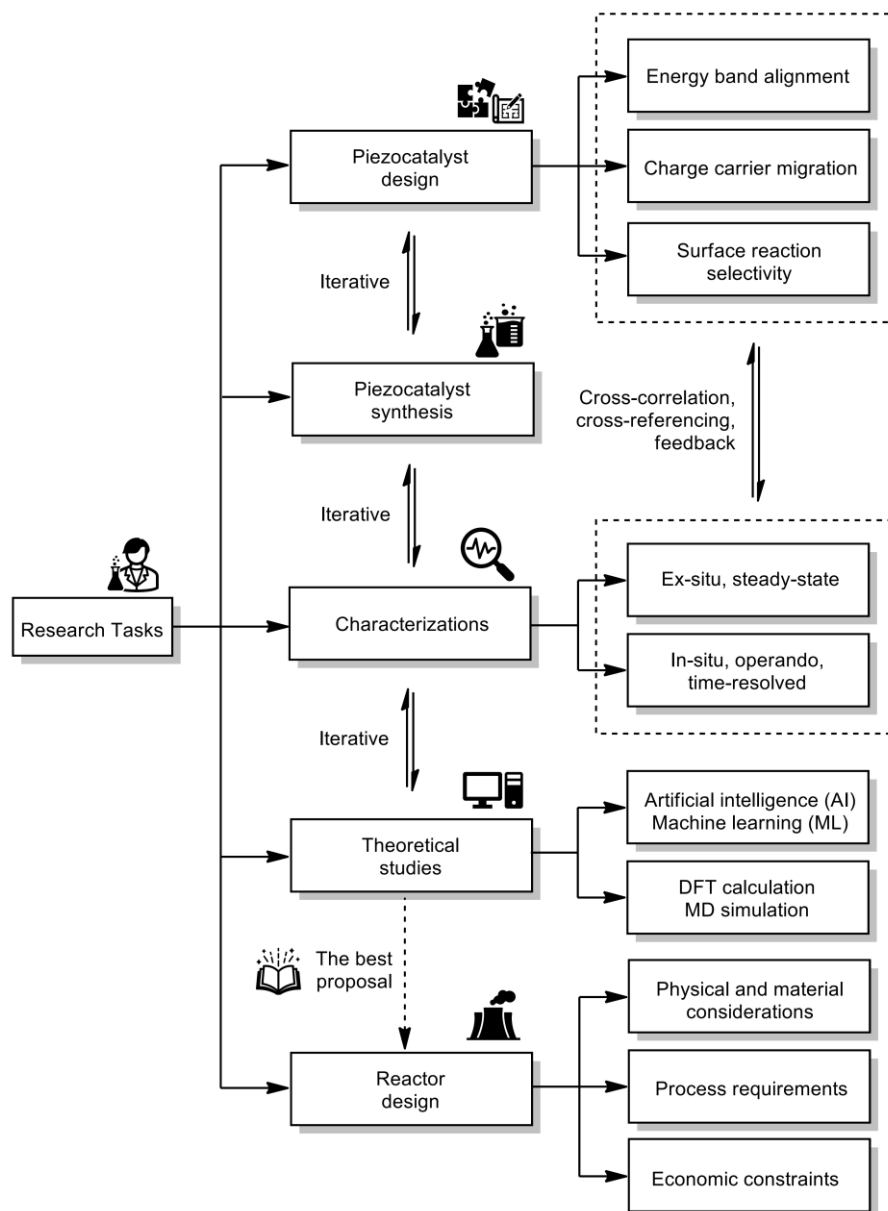


**Figure 5.** Schematic illustration of the research tasks aimed at developing highly active piezocatalysts and translating laboratory-scale achievements to further steps.

## 8. Outlook

Despite the progress made in utilizing piezoelectric materials for redox reactions, piezocatalyzed organic transformations are still in their infancy. Therefore, challenges remain that must be overcome in order to fully harness their potential. One of the primary challenges is the efficient transfer of mechanical energy to the piezoelectric material to generate sufficient electrochemical potential for redox activation. The efficiency of energy transfer can be affected by factors such as the particle size of the piezoelectric material, the frequency and amplitude of mechanical agitation, and the presence of any liquid or solid additives. Unlike the more mature field of photoredox catalysis, establishing a clear relationship between the energy transfer from the mechanical energy source, the mass transfer of reactants from the bulk to the catalyst surface, charge transfer

within the catalyst and to adsorbed species, and the resulting catalytic performance in piezoredox catalysis remains challenging. This difficulty arises due to the absence of in-situ and operando characterization techniques that can operate under mechanical force. Readers should be aware that the terms in-situ and operando, which are occasionally used interchangeably, are distinct. In-situ characterization examines materials under conditions that replicate their actual application environment, such as temperature, pressure, or mechanical force, without directly monitoring their performance during the process. In contrast, operando characterization simultaneously observes the structure and properties of the material while measuring its performance under working conditions. Thus, in-situ focuses on environmental mimicking, while operando goes further by combining this with real-time performance evaluation.

Another challenge is the relatively narrow range of reactions that have been demonstrated using piezoredox catalysis. Further research is needed to expand the scope of piezoredox reactions to include a broader range of substrates and bond-forming processes. This expansion will require a deeper understanding of the underlying mechanisms and the development of new piezoelectric materials with tailored properties. For example, one limitation of using piezoelectric materials as photoredox catalyst mimics is their reliance on diazonium salts as aryl radical precursors. To compete with piezocatalytic method, the Chen group in 2025 developed a mechanochemical method for synthesizing chalcogenoacetylenes (alkynyl selenides and alkynyl tellurides) using alkynyl sulfonium salts as precursors.<sup>80</sup> This approach, enabled by a charge transfer complex, provides a versatile and efficient pathway for generating alkynyl radicals under solvent- and metal-free conditions. Using NaI as an electron donor and ethyl acetate as a LAG additive, the method achieves high yields (up to 95%) within 30 min of milling in air. Broad substrate compatibility was also demonstrated, accommodating a range of diselenides, ditellurides, and alkynyl sulfonium salts with yields between 61–89%, and aligns with green chemistry principles, requiring no inert gas protection, minimizing solvent use, and operating under mild conditions. Indeed, although Chen's method provides a straightforward alternative to the piezocatalyzed reactions, it has a drawback: the electron donor, NaI, is consumed during the reaction and cannot be reused, unlike the reusable piezoelectric materials. Thus, for the piezocatalysis route to remain competitive, the limitation of relying on diazonium salts must be addressed.

The scalability of piezoredox reactions also poses challenges for practical applications. Although laboratory-scale reactions have yielded promising results, scaling up these processes to an industrial level is difficult, especially in ensuring consistent mechanical agitation and energy input. In addition, laboratory yields typically range from milligram to gram scales, whereas industrial applications require kilogram to ton-scale yields, highlighting a huge discrepancy. The development of scalable reactor designs that can effectively utilize piezoelectric materials for large-scale redox reactions is an area of ongoing research. Future research should focus on the development of new piezoelectric materials with enhanced properties, such as higher sensitivity to low-frequency mechanical forces, higher piezoelectric coefficients, improved stability, and greater compatibility with a broader range of organic substrates.

As a starting point, commercially available piezoelectric materials with proven photocatalytic activity, such as BaTiO<sub>3</sub> and ZnO, can be used. These pristine materials can be further improved by altering their electronic properties, such as through doping with impurity ions, to achieve better performance. ZnO, for example, has been extensively studied as a catalyst in the more established field of photocatalysis. The knowledge gained from optimizing its performance and best practices in photocatalysis can be adapted and refined for piezocatalysis. Indeed, piezocatalysis is more complex than photocatalysis, especially when conducted in solution, since sonochemical aspects and the physicochemical properties of the solvent play a role in the transformation of reactants to products. In-depth studies are required to unravel the detailed mechanisms underlying piezoelectric-induced redox reactions, with particular emphasis on the roles of surface

charge dynamics, material structure, solvent properties, and the influence of additives. To this end, the construction of operando characterization setups tailored specifically for piezocatalytic reactions emerges as an important step forward.

An exciting area of future research is the integration of piezoelectric materials with other forms of energy input, such as light or electrical fields, to create hybrid catalytic systems that can achieve unprecedented levels of control and selectivity in chemical reactions especially when using ultrasound as the source of mechanical energy. These hybrid systems could offer new strategies for driving complex multi-step reactions, where different types of energy inputs are used to selectively activate specific intermediates or pathways.

Altogether, the broader adoption of piezoelectric materials for redox reactions could potentially transform the chemical industry by enabling more sustainable and efficient methods for synthesizing value-added chemicals, facilitating the formation of chemical bonds in organic substrates with improved kinetics, and activating small molecules to become energy carriers. By reducing the reliance on toxic reagents and organic solvents, piezoredox catalysis aligns with the principles of green chemistry and offers a pathway toward more environmentally friendly chemical processes. The development of scalable piezoredox technologies could enable new applications in areas such as drug discovery, material science, and renewable energy, further broadening the impact of this innovative approach.

## 9. Conclusions

Piezoredox catalysis represents a new paradigm in chemical synthesis, offering a promising alternative to traditional redox and photoredox catalysis. By harnessing the unique properties of piezoelectric materials to mediate redox reactions under mechanical stress, piezoredox catalysis integrates the benefits of sonochemistry, mechanochemistry, and heterogeneous catalysis. The simplicity and potential scalability of piezoredox methods make them appealing for large-scale applications, where sustainability and efficiency need to be considered together. Although still in its early stages, piezoredox catalysis holds promise for further development and innovation, particularly in expanding the scope of redox transformations. As research in this area continues to progress, piezoredox catalysis is poised to play a pivotal role in advancing new synthetic methodologies and promoting more sustainable practices in industrial settings.

## Acknowledgements

This work was supported by NAWA (Narodowa Agencja Wymiany Akademickiej) under Grant Number BPN/ULM/2022/1/00009.

## References

1. J. A. Leitch and D. L. Browne, *Chemistry—A European Journal*, 2021, **27**, 9721-9726.  
<https://doi.org/10.1002/chem.202100348>
2. S. Tu, Y. Guo, Y. Zhang, C. Hu, T. Zhang, T. Ma and H. Huang, *Advanced Functional Materials*, 2020, **30**, 2005158.

- <https://doi.org/10.1002/adfm.202005158>
3. H. Xia and Z. Wang, *Science*, 2019, **366**, 1451-1452.  
<https://doi.org/10.1126/science.aaz9758>
  4. R. F. Martínez, G. Cravotto and P. Cintas, *The Journal of Organic Chemistry*, 2021, **86**, 13833-13856.  
<https://doi.org/10.1021/acs.joc.1c00805>
  5. D. Tan and T. Friščić, *European Journal of Organic Chemistry*, 2018, **2018**, 18-33.  
<https://doi.org/10.1002/ejoc.201700961>
  6. E. M. Marrero, C. J. Caprara, C. N. Gilbert, E. E. Blanco and R. G. Blair, *Faraday Discussions*, 2023, **241**, 91-103.  
<https://doi.org/10.1039/D2FD00084A>
  7. S. M. Zeitler and M. R. Golder, *Chemical Communications*, 2024, **60**, 26-35.  
<https://doi.org/10.1039/D3CC04323A>
  8. S. Jiang and M. Wang, *Current Organic Chemistry*, 2024, **28**, 905-913.  
<https://doi.org/10.2174/0113852728306541240409034052>
  9. H. Sudrajat, I. Rossetti, I. Carra and J. C. Colmenares, *Current Opinion in Chemical Engineering*, 2024, **45**, 101043.  
<https://doi.org/10.1016/j.coche.2024.101043>
  10. H. Sudrajat, I. Rossetti and J. C. Colmenares, *Journal of Materials Chemistry A*, 2023, **11**, 24566-24590.  
<https://doi.org/10.1039/D3TA04758J>
  11. G. Cravotto, E. C. Gaudino and P. Cintas, *Chemical Society Reviews*, 2013, **42**, 7521-7534.  
<https://doi.org/10.1039/c2cs35456j>
  12. P. A. May and J. S. Moore, *Chemical Society Reviews*, 2013, **42**, 7497-7506.  
<https://doi.org/10.1039/c2cs35463b>
  13. H. Zheng, Y. Wang, J. Liu, K. Yan and K. Zhu, *Applied Catalysis B: Environmental*, 2024, **341**, 123335.  
<https://doi.org/10.1016/j.apcatb.2023.123335>
  14. K. Wang, C. Han, J. Li, J. Qiu, J. Sunarso and S. Liu, *Angewandte Chemie*, 2022, **134**, e202110429.  
<https://doi.org/10.1002/ange.202110429>
  15. M. H. Shaw, J. Twilton and D. W. MacMillan, *The Journal of organic chemistry*, 2016, **81**, 6898-6926.  
<https://doi.org/10.1021/acs.joc.6b01449>
  16. K.-S. Hong, H. Xu, H. Konishi and X. Li, *The Journal of Physical Chemistry letters*, 2010, **1**, 997-1002.  
<https://doi.org/10.1021/jz100027t>
  17. H. Mohapatra, M. Kleiman and A. P. Esser-Kahn, *Nature Chemistry*, 2017, **9**, 135-139.  
<https://doi.org/10.1038/nchem.2633>
  18. H. Mohapatra, J. Ayarza, E. C. Sanders, A. M. Scheuermann, P. J. Griffin and A. P. Esser-Kahn, *Angewandte Chemie International Edition*, 2018, **57**, 11208-11212.  
<https://doi.org/10.1002/anie.201804451>
  19. Z. Wang, J. Ayarza and A. P. Esser-Kahn, *Angewandte Chemie*, 2019, **131**, 12151-12154.  
<https://doi.org/10.1002/ange.201903956>
  20. Z. Wang, X. Pan, L. Li, M. Fantin, J. Yan, Z. Wang, Z. Wang, H. Xia and K. Matyjaszewski, *Macromolecules*, 2017, **50**, 7940-7948.  
<https://doi.org/10.1021/acs.macromol.7b01597>
  21. Z. Wang, X. Pan, J. Yan, S. Dadashi-Silab, G. Xie, J. Zhang, Z. Wang, H. Xia and K. Matyjaszewski, *ACS Macro Letters*, 2017, **6**, 546-549.  
<https://doi.org/10.1021/acsmacrolett.7b00152>

22. J. Yoon, J. Kim, F. Tieves, W. Zhang, M. Alcalde, F. Hollmann and C. B. Park, *ACS Catalysis*, 2020, **10**, 5236-5242.  
<https://doi.org/10.1021/acscatal.0c00188>
23. K. Kubota, Y. Pang, A. Miura and H. Ito, *Science*, 2019, **366**, 1500-1504.  
<https://doi.org/10.1126/science.aay8224>
24. Y. Pang, J. W. Lee, K. Kubota and H. Ito, *Angewandte Chemie International Edition*, 2020, **59**, 22570-22576.  
<https://doi.org/10.1002/anie.202009844>
25. C. Schumacher, J. G. Hernández and C. Bolm, *Angewandte Chemie International Edition*, 2020, **59**, 16357-16360.  
<https://doi.org/10.1002/anie.202003565>
26. Y. Wang, Z. Zhang, L. Deng, T. Lao, Z. Su, Y. Yu and H. Cao, *Organic Letters*, 2021, **23**, 7171-7176.  
<https://doi.org/10.1021/acs.orglett.1c02575>
27. G. Wang, J. Jia, Y. He, D. Wei, M. Song, L. Zhang, G. Li, H. Li and B. Yuan, *RSC Advances*, 2022, **12**, 18407-18411.  
<https://doi.org/10.1039/D2RA02255A>
28. H. Lv, X. Xu, J. Li, X. Huang, G. Fang and L. Zheng, *Angewandte Chemie*, 2022, **134**, e202206420.
29. J. Jiang, S. Song, J. Guo, J. Zhou and J. Li, *Tetrahedron Letters*, 2022, **98**, 153820.  
<https://doi.org/10.1016/j.tetlet.2022.153820>
30. F. Liu, L. N. Chen, A. M. Chen, Z. P. Ye, Z. W. Wang, Z. L. Liu, X. C. He, S. H. Li and P. J. Xia, *Advanced Synthesis & Catalysis*, 2022, **364**, 1080-1084.  
<https://doi.org/10.1002/adsc.202101293>
31. L. Song, T. Zhang, S. Zhang, J. Wei and E. Chen, *ACS Sustainable Chemistry & Engineering*, 2022, **10**, 5129-5137.  
<https://doi.org/10.1021/acssuschemeng.1c08412>
32. Y. He, G. Wang, W. Hu, D. Wei, J. Jia, H. Li and B. Yuan, *ACS Sustainable Chemistry & Engineering*, 2023, **11**, 910-920.  
<https://doi.org/10.1021/acssuschemeng.2c04720>
33. R. Ding, Q. Liu and L. Zheng, *Chemistry—A European Journal*, 2023, **29**, e202203792.  
<https://doi.org/10.1002/chem.202203792>
34. H. Wang, W. Ding and G. Zou, *The Journal of Organic Chemistry*, 2023, **88**, 12891-12901.  
<https://doi.org/10.1021/acs.joc.3c00681>
35. M. Huang, L. Deng, T. Lao, Z. Zhang, Z. Su, Y. Yu and H. Cao, *The Journal of Organic Chemistry*, 2024, **89**, 9733-9743.  
<https://doi.org/10.1021/acs.joc.3c02404>
36. X. Wang, X. Zhang, X. He, G. Guo, Q. Huang, F. You, Q. Wang, R. Qu, F. Zhou and Z. Lian, *Angewandte Chemie International Edition*, 2024, **63**, e202410334.  
<https://doi.org/10.1002/anie.202410334>
37. S.-L. Niu, W. Yuan, X. Gong, B. Bao, Z.-W. Wu, B. Xu, R. Zeng, Q.-W. Yang and Q. Ouyang, *ACS Sustainable Chemistry & Engineering*, 2023, **11**, 17816-17825.  
<https://doi.org/10.1021/acssuschemeng.3c06118>
38. P. Chakma, S. M. Zeitler, F. Baum, J. Yu, W. Shindy, L. D. Pozzo and M. R. Golder, *Angewandte Chemie*, 2023, **135**, e202215733.  
<https://doi.org/10.1002/ange.202215733>
39. M. R. Andrews, C. Collet, A. Wolff and C. Hollands, *Propellants, Explosives, Pyrotechnics*, 2020, **45**, 77-86.

<https://doi.org/10.1002/prep.201900280>

40. F. Effaty, L. Gonnet, S. G. Koenig, K. Nagapudi, X. Ottenwaelder and T. Frišćić, *Chemical Communications*, 2023, **59**, 1010-1013.  
<https://doi.org/10.1039/D2CC06013B>
41. C. B. Lennox, T. H. Borchers, L. Gonnet, C. J. Barrett, S. G. Koenig, K. Nagapudi and T. Frišćić, *Chemical science*, 2023, **14**, 7475-7481.  
<https://doi.org/10.1039/D3SC01591B>
42. L. Gonnet, C. B. Lennox, J. L. Do, I. Malvestiti, S. G. Koenig, K. Nagapudi and T. Frišćić, *Angewandte Chemie International Edition*, 2022, **61**, e202115030.  
<https://doi.org/10.1002/anie.202115030>
43. H. G. Roth, N. A. Romero and D. A. Nicewicz, *Synlett*, 2016, **27**, 714-723.  
<https://doi.org/10.1055/s-0035-1561297>
44. M. Rafiee, D. J. Abrams, L. Cardinale, Z. Goss, A. Romero-Arenas and S. S. Stahl, *Chemical Society Reviews*, 2024, **53**, 566-585.  
<https://doi.org/10.1039/D2CS00706A>
45. J. Lodh, S. Paul, H. Sun, L. Song, W. Schöffberger and S. Roy, *Frontiers in Chemistry*, 2023, **10**, 956502.  
<https://doi.org/10.3389/fchem.2022.956502>
46. S. Wang, J. Zhang, O. Gharbi, V. Vivier, M. Gao and M. E. Orazem, *Nature Reviews Methods Primers*, 2021, **1**, 41.  
<https://doi.org/10.1038/s43586-021-00039-w>
47. Y. Zhai, Z. Zhu, S. Zhou, C. Zhu and S. Dong, *Nanoscale*, 2018, **10**, 3089-3111.  
<https://doi.org/10.1039/C7NR07803J>
48. R. Fedorov and G. Gryn'ova, *Journal of Chemical Theory and Computation*, 2023, **19**, 4796-4814.  
<https://doi.org/10.1021/acs.jctc.3c00355>
49. N. Kvasovs and V. Gevorgyan, *Chemical Society Reviews*, 2021, **50**, 2244-2259.  
<https://doi.org/10.1039/D0CS00589D>
50. N. J. Treat, H. Sprafke, J. W. Kramer, P. G. Clark, B. E. Barton, J. Read de Alaniz, B. P. Fors and C. J. Hawker, *Journal of the American Chemical Society*, 2014, **136**, 16096-16101.  
<https://doi.org/10.1021/ja510389m>
51. Á. Péter, S. Agasti, O. Knowles, E. Pye and D. J. Procter, *Chemical Society Reviews*, 2021, **50**, 5349-5365.  
<https://doi.org/10.1039/D0CS00358A>
52. C. M. Hendy, G. C. Smith, Z. Xu, T. Lian and N. T. Jui, *Journal of the American Chemical Society*, 2021, **143**, 8987-8992.  
<https://doi.org/10.1021/jacs.1c04427>
53. S. Hosseini, J. N. Janusz, M. Tanwar, A. D. Pendergast, M. Neurock and H. S. White, *Journal of the American Chemical Society*, 2022, **144**, 21103-21115.  
<https://doi.org/10.1021/jacs.2c07305>
54. M. Jonsson, D. D. Wayner and J. Lusztyk, *The Journal of Physical Chemistry*, 1996, **100**, 17539-17543.  
<https://doi.org/10.1021/jp961286q>
55. Y. Wang, P. Hu, J. Yang, Y.-A. Zhu and D. Chen, *Chemical Society Reviews*, 2021, **50**, 4299-4358.  
<https://doi.org/10.1039/D0CS01262A>
56. C. Schotten, T. P. Nicholls, R. A. Bourne, N. Kapur, B. N. Nguyen and C. E. Willans, *Green Chemistry*, 2020, **22**, 3358-3375.  
<https://doi.org/10.1039/D0GC01247E>

57. N. Bhadwal, R. Ben Mrad and K. Behdinin, *Sensors*, 2023, **23**, 3859.  
<https://doi.org/10.3390/s23083859>
58. Z. Wang, J. Hu, A. P. Suryavanshi, K. Yum and M.-F. Yu, *Nano Letters*, 2007, **7**, 2966-2969.  
<https://doi.org/10.1021/nl070814e>
59. S. S. Tripathy and A. M. Raichur, *Journal of Experimental Nanoscience*, 2011, **6**, 127-137.  
<https://doi.org/10.1080/17458080.2010.483695>
60. P. Wu, P. Cui, H. Du, M. E. Alves, C. Liu, D. Zhou and Y. Wang, *ACS Earth and Space Chemistry*, 2019, **3**, 495-502.  
<https://doi.org/10.1021/acsearthspacechem.8b00165>
61. T. Takata, J. Jiang, Y. Sakata, M. Nakabayashi, N. Shibata, V. Nandal, K. Seki, T. Hisatomi and K. Domen, *Nature*, 2020, **581**, 411-414.  
<https://doi.org/10.1038/s41586-020-2278-9>
62. Sukesha, R. Vig and N. Kumar, *Integrated Ferroelectrics*, 2015, **167**, 154-175.  
<https://doi.org/10.1080/10584587.2015.1107383>
63. W. Jiang, R. Zhang, B. Jiang and W. Cao, *Ultrasonics*, 2003, **41**, 55-63.  
[https://doi.org/10.1016/S0041-624X\(02\)00436-5](https://doi.org/10.1016/S0041-624X(02)00436-5)
64. Z. Liu, H. Wu, Y. Yuan, H. Wan, Z. Luo, P. Gao, J. Zhuang, J. Zhang, N. Zhang and J. Li, *Current Opinion in Solid State and Materials Science*, 2022, **26**, 101016.  
<https://doi.org/10.1016/j.cossms.2022.101016>
65. D. Hu, M. Yao, Y. Fan, C. Ma, M. Fan and M. Liu, *Nano Energy*, 2019, **55**, 288-304.  
<https://doi.org/10.1016/j.nanoen.2018.10.053>
66. B. Mortazavi, B. Javvaji, F. Shojaei, T. Rabczuk, A. V. Shapeev and X. Zhuang, *Nano Energy*, 2021, **82**, 105716.  
<https://doi.org/10.1016/j.nanoen.2020.105716>
67. H. D. Espinosa, R. A. Bernal and M. Minary-Jolandan, *Advanced Materials*, 2012, **24**, 4656-4675.  
<https://doi.org/10.1002/adma.201104810>
68. S. Bai, N. Zhang, C. Gao and Y. Xiong, *Nano Energy*, 2018, **53**, 296-336.  
<https://doi.org/10.1016/j.nanoen.2018.08.058>
69. A. J. Medford, A. Vojvodic, J. S. Hummelshøj, J. Voss, F. Abild-Pedersen, F. Studt, T. Bligaard, A. Nilsson and J. K. Nørskov, *Journal of Catalysis*, 2015, **328**, 36-42.  
<https://doi.org/10.1016/j.jcat.2014.12.033>
70. Y. Wang, X. Guo, L. H. Li, J. Zhang, G. K. Li, A. Zavabeti and Y. Li, *ACS Applied Nano Materials*, 2022, **5**, 12126-12142.  
<https://doi.org/10.1021/acsanm.2c01871>
71. X. Li, M. Sun, X. Wei, C. Shan and Q. Chen, *Nanomaterials*, 2018, **8**, 188.  
<https://doi.org/10.3390/nano8040188>
72. Y. Liu, H.-Y. Xu and S. Komarneni, *Applied Catalysis A: General*, 2023, 119550.  
<https://doi.org/10.1016/j.apcata.2023.119550>
73. X. Luo, Q. Li and Y. Wang, *Materials*, 2024, **17**, 844.  
<https://doi.org/10.3390/ma17040844>
74. S.-D. Kim, G.-T. Hwang, K. Song, C. K. Jeong, K.-I. Park, J. Jang, K.-H. Kim, J. Ryu and S.-Y. Choi, *Nano Energy*, 2019, **58**, 78-84.  
<https://doi.org/10.1016/j.nanoen.2018.12.096>

75. Z. Wang, X. Pan, Y. He, Y. Hu, H. Gu and Y. Wang, *Advances in Materials Science and Engineering*, 2015, **2015**, 165631.  
<https://doi.org/10.1155/2015/165631>
76. V. Consonni and A. M. Lord, *Nano Energy*, 2021, **83**, 105789.  
<https://doi.org/10.1016/j.nanoen.2021.105789>
77. C. An, H. Qi, L. Wang, X. Fu, A. Wang, Z. L. Wang and J. Liu, *Nano Energy*, 2021, **82**, 105653.  
<https://doi.org/10.1016/j.nanoen.2020.105653>
78. H. Jiang, L. Song, Z.-X. Huang, M. Liu, Y. Zhao, S. Zhang, J. Guo, Y. Li, Q. Wang and J.-P. Qu, *Nano Energy*, 2022, **104**, 107921.  
<https://doi.org/10.1016/j.nanoen.2022.107921>
79. J. A. Krishnaswamy, F. C. Buroni, F. Garcia-Sanchez, R. Melnik, L. Rodriguez-Tembleque and A. Saez, *Composite Structures*, 2019, **224**, 111033.  
<https://doi.org/10.1016/j.compstruct.2019.111033>
80. F. Tan, C.-Z. Fang, B.-S. Qiu, H. Sheng, Y.-L. Tu and X.-Y. Chen, *Organic Chemistry Frontiers*, 2025, **Advance Article**.

## Authors' Biographies



**Hanggara Sudrajat** is a tenured researcher at National Research and Innovation Agency of Indonesia (BRIN). He graduated cum laude from Universitas Gadjah Mada before beginning his career in the chemicals industry. He later earned his PhD in catalysis from Thammasat University in 2016, completing his PhD research at the University of Tokyo. He received the Best Doctoral Thesis Award in Science and Technology. Following his PhD, he joined Kobe University as a JSPS postdoctoral fellow. After a brief tenure at TU Eindhoven, he moved to BRIN. He was also a NAWA postdoctoral fellow at the Polish Academy of Sciences. His research interests focus on charge-carrier-based catalysis and advanced spectroscopy.



**Juan Carlos Colmenares** graduated from Warsaw University of Technology (Chem. Eng. 1995) and obtained his M.Sc. (1997) in catalysis for organic technology and Ph.D. (2004) in chemical and material sciences from the same university, the scientific degree of habilitation (D.Sc. 2015) from the Institute of Physical Chemistry of the Polish Academy of Sciences in Poland, and in 2023 Full Professor in Chemical Sciences given by the Council of Excellence in Poland/Office of the President of Poland. His interests range from materials science, nanotechnology, and heterogeneous catalysis to biomass or CO<sub>2</sub> valorization, solar chemicals, sonication, photocatalysis, and water or air purification. After obtaining his Ph.D., he worked at the University of Córdoba, Spain (2005–2006) in Prof. Marinas' group as a postdoctoral fellow, and at the University of Southern California, Los Angeles (USA) (2006–2009) in Prof. G. A. Olah's (Nobel Prize in Chemistry) group as a postdoctoral research associate. He is a Marie Skłodowska-Curie fellow. He serves as an expert evaluator for many important scientific journals and institutions and chemical companies, and as a member of the editorial advisory board for Scientific Reports and Molecules (Photochemistry Section) journals. He has coauthored more than 150 works published in international scientific journals and books and filed seven patent applications (five accepted). Presently, he is working as full professor at the Institute of Physical Chemistry of the Polish Academy of Sciences in Poland.

This paper is an open access article distributed under the terms of the Creative Commons Attribution (CC BY) license (<http://creativecommons.org/licenses/by/4.0/>)